ALMA MATER STUDIORUM - UNIVERSITY OF BOLOGNA

SCHOOL OF ENGINEERING AND ARCHITECTURE

Department of Electrical, Electronic and Information Engineering "Guglielmo Marconi" - DEI

MASTER'S DEGREE IN AUTOMATION ENGINEERING

Graduation Thesis in

Automatic Machine Design and Control

Development of a Kinetic Energy Recovery System for a Rotary Turret Machine

Author:
Gabriele Yunes Daoudi

Supervisor:
Eminent Prof. Andrea Tilli
Co-Supervisor:
Ing. Jacopo Cassoli
Ing. Pierluigi Tadeo
Gianluca Baraldi

October 5, 2018

Academic Year 2017/2018
Graduation Session II

Abstract

Development of a Kinetic Energy Recovery System for a Rotary Turret Machine

The scope of the Kinetic Energy Recovering Systems is to store a certain amount of energy during the system's nominal operation by recovering it from the brakes and reuse it later.
The scope of this thesis will be studied the development of such system on an automatic machine. The field of application is known as "Green Automation", that became popular during the last decade.
The machine analyzed is a rotary turret one that operates in the beverage automation. Its role is to apply a particular type of cap on the cans to improve the hygiene and the aesthetics.
The problem has been tackled by elaborating mathematical models of the physical systems, performing different tests and data logging, applying Parameter Identification Algorithms and finally developing the solution. It has been also performed a brief analysis of the different available technologies to realize the system.The project has been validated performing simulations on the models.

Studio di Sistema di Recupero di Energia Cinetica per una Macchina a Giostra Rotativa

Lo scopo dei sistemi di recupero di energia cinetica è quello di accumulare una certa quantità di energia durante il funzionamento nominale di un sistema per riutilizzarla in seguito.
Lo scopo di questa tesi è quello di studiare lo sviluppo di un sistema simile per una macchina automatica. Il campo di applicazione è noto come "Green Automation", divenuto molto popolare nell'ultima decade.
La macchina analizzata ha una struttura a giostra rotativa e opera nel campo dell'automazione per il beverage. Il suo scopo è quello di applicare una capsula sulle lattine per motivi igienici ed estetici.
Il problema è stato affrontato elaborando modelli matematici per i sistemi fisici, eseguendo diversi test registrandone i dati, applicando algoritmi di identificazione parametrica ed infine sviluppando il sistema finale. È stata inoltre eseguita una breve analisi sulle diverse tecnologie disponibili per la realizzazione del sistema. Il progetto è stato validato tramite simulazioni applicate ai modelli.

Contents

0.1 Chapters Introduction

- **Introduction:**
  The Introduction chapter describes the main objectives of the Thesis and its environment. An explanation has been provided regarding the steps that have been performed during the development of the project in order to achieve them.

- **Machine Description:**
  The Machine Description chapter is a brief description of the system involved during the Thesis and some important operations that the system performs while working that are relevant for the Thesis's course.

- **Physical Modeling:**
  This chapter is a deep description of the mathematical representation adopted in order to represent the system and all its parameters, including the instruments that have been used to develop it.

- **Resistive Torque Modeling:**
  The Resistive Torque Modeling chapter explains all the different tests that have been performed on the system with the scope to estimate some parameters. Furthermore, the data comings from these tests have been used to validate the built model. Some comments on the results conclude the tests section.

- **System Realization:**
  This chapter explains the different technologies that have been analyzed in order to develop the technical solution needed by the machine. It is also described the final solution adopted with the relative sizing procedure.

- **System Control:**
  In this chapter are described different control approaches, highlighting the pro and cons of each one and the definition of the final control strategy.

- **Conclusion:**
  This final chapter compares the developed solution with the now applied one focusing on the benefits gained with the new system.

Chapter 1

Introduction

1.1 Introduction

This thesis has been developed in collaboration with the company Ecocap's S.r.l. situated in Casalecchio di Reno (BO). The field is strictly related with the automation and in particular with automatic machines design.
All the development of the project has been performed at Ecocap's headquarter by the master's candidate in collaboration with the internal technical office.

The project has been proposed with the aim of developing a Kinetic Energy Recovery System(KERS) that could be applied on a particular type of machine produced by Ecocap's. The aim of this KERS is to store as much as possible kinetic energy recovered during the nominal operation of the machine and then provide to a secondary power supply in the case that the main supply (coming from the grid) shuts down.
When there is a blackout, there is a succession of phases that provide the emptying of the machine since if the products remain inside it, they will cause a chain of damage.

Before the thesis project, this system was realized by using an UPS System that has to be charged from the grid separately. The secondary scope of the thesis is infact to replace this UPS unity with a more "green" and efficent system.

FIGURE 1.1: UPS Group actually used

1.2 Method adopted

For the energy recovering has been taken into account only the groups that at nominal conditions have some braking with a consequent energy dissipation. Other motors, as will be explained, brake only to adjust the machine velocity with respect to the feed flow of products. For this reason, the nominal condition has been considered as the worst one for the energy recovery.

The project has been divided into phases that have been followed chronologically. Main phases:

- **Machine analysis as a whole system:**
  This phase was necessary in order to understand the structure, type of motors and main characteristic of the machine. During this phase it has been identified which motors to take into account for the energy recovery and the mechanism involved during the emptying phase.

- **Physical modeling of the mechanism related to the energy recovery system:**
  During this phase it has been modeled all the machine's groups under the mechanical and electrical point of views. In order to develop this task, it has been used Matlab Simulink and Simscape toolbox for the physical modeling.

- **Experimental test to estimate some unknown parameters:**
  This phase of the thesis has been performed in order to estimate, from physical data, some a priori unknown parameters. For example, the friction parameters are the most important ones that have been estimated from these tests.
  The development of these tests has been performed by an Ecocap's engineer under the intern's directions.

- **Validation of the model with simulation and experimental data:** The phase following the experimental tests is the one in order to validate the previously built models. In this phase various simulations have been performed with the scope to adjust, if necessary, the parameters coming from some previous knowledge as the Mechanical CAD.
  Moreover,it has ben provided a simulation of the machine behaviour both during the nominal condition and the emptying phase. This is done in order to estimate respectively the energy flux coming back from the machine and the total amount of energy necessary for the emptying phase.

- **Develop of control strategy for the KERS:**
  The last phase of the thesis is the development of an efficient control strategy both for the energy accumulation phase and the energy reutilization phase.

The following chapters are divided explaining these different phases.

Chapter 2

MachineDescription

2.1 Machine Description

The machine is referred as Ecocap's CSS648. Its function is to apply an aluminum cap on a can to preserve the hygienity.
To apply the cap, it is necessary to press it with a given pressure at a given temperature for a precise time.
If the time is exceeded, the can (independently from the liquid inside) will explode causing an immediate crystallization of sugars. As consequence, the machine needs a long maintenance phase for clean all the mechanical parts involved.

The machine has a rotary structure with a continuous motion approach in order to reach the maximum productivity level of 55000 can/hour.

The aim of the KERS is to provide an emergency power supply in order to stop the coming flow of cans and emptying the machine from the cans inside. As previously said, this operation is now performed by a UPS Unit.

The machine is divided into 5 main groups:

- Infeed Screw
- Infeed/Outfeed Carousels
- Main Turret
- 4x Lids Transfers
- 4x Lids PickUps

These groups are analyzed in detail in the following.

Infeed Screw

The role of the Infeed Screw is to put in step the product(cans) with the following Infeed Carousel. In particular the screw produces an acceleration of the cans thanks to the increasing screw pitch.

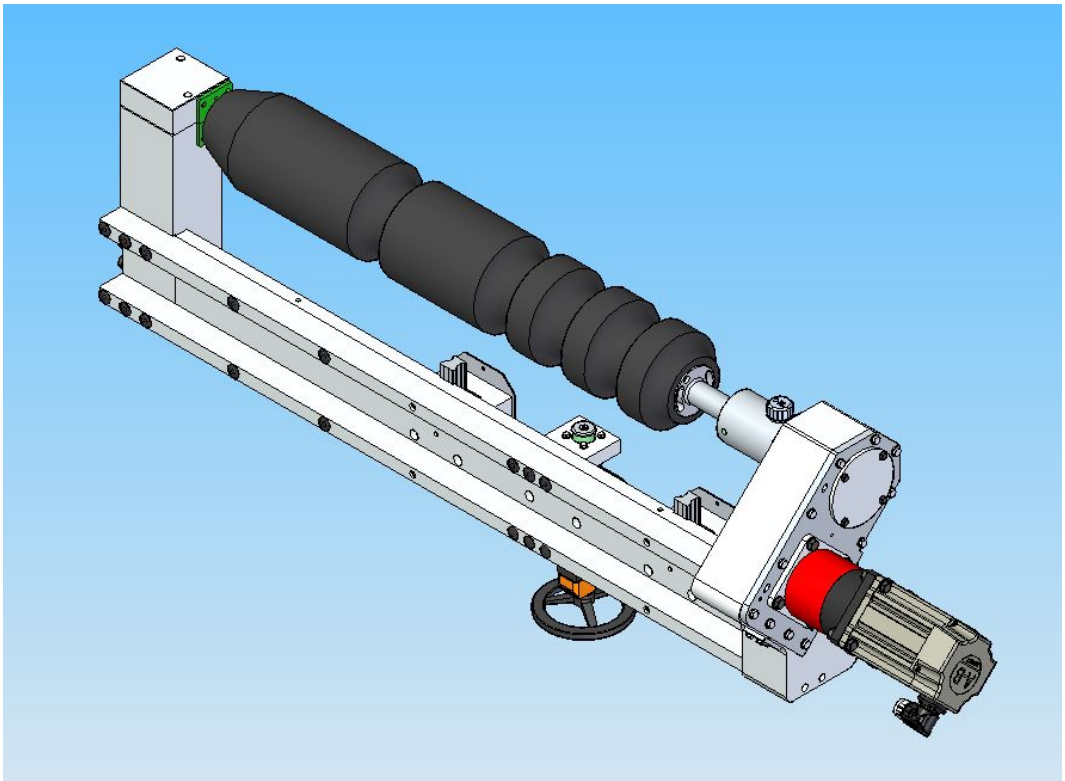

FIGURE 2.1: Cad representation of Screw group

The cans come on a conveyor belt at a given speed and the Screw needs to be Synchronized both with the conveyor and the carousel. The synchronization is made by a virtual master that is phased with respect to the Main Turret.

The main problem related to the Screw is that for stop the incoming flow of cans, it's necessary to reach an "Emptying Velocity" of not more than 20000 cans/hour. If that bond is not satisfied, there will remain a "Floating Can" in between to the Belt and the Screw. Consequently, that can can be destroyed causing damages to all the following groups.

The main component is composed by a PVC screw that can accelerate the can without damage it.

Infeed/Outfeed Carousel

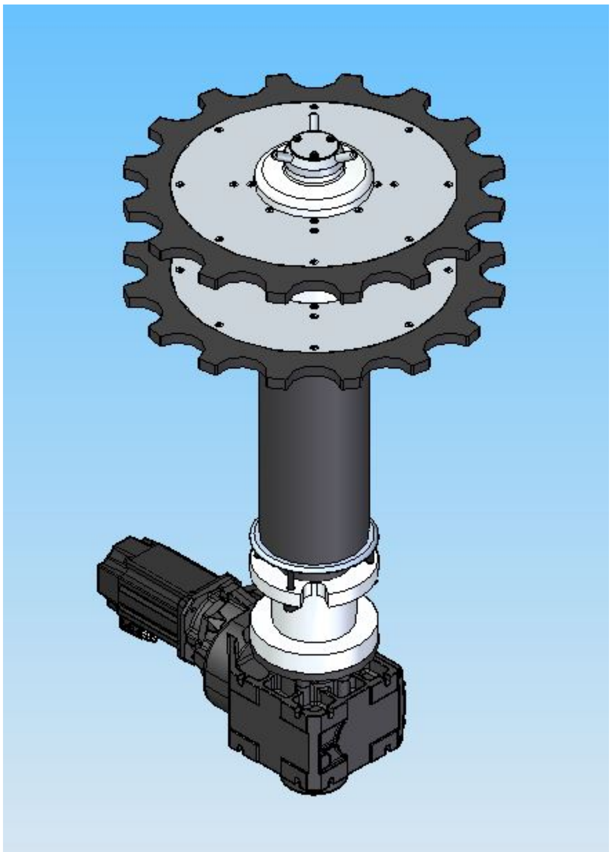

FIGURE 2.2: Cad representation of Carousel group

The two Carousels are mechanically twins and are placed respectively in input and in output of the Main Turret.
Their role is to correctly switch the product from the Screw to the Main Turret and from the Main Turret to the Output Conveyor Belt. This is necessary since the rotation of the Main Turret is in the opposite direction with respect to the velocities of the incoming/outcoming flows of products.

Since they are exactly the same mechanism, during the thesis will be considered only a generic Carousel.
The Synchronization of the two Carousels is made by a virtual master that is phased with respect to the main turret's master.

Main Turret

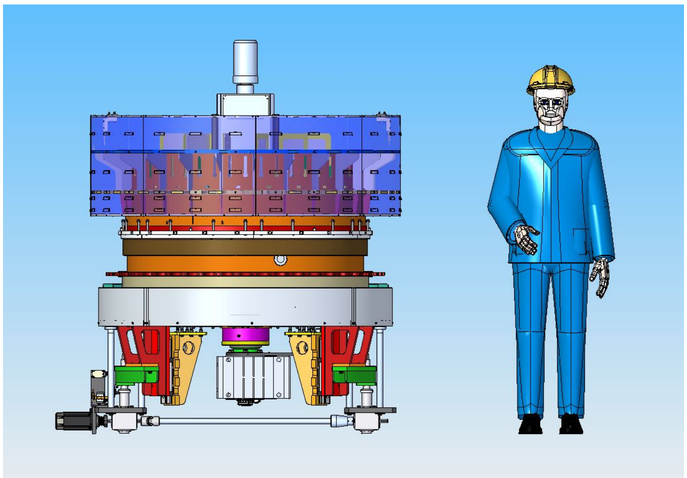

FIGURE 2.3: Cad representation of Main Turret group

The Main Turret is the group that physically applies the caps on the cans. This operation is performed using a particular type of Heating Heads that catch the cans, apply a pressure thanks to a mechanical cam, holds the cans for few seconds and then release them to the Outfeed Carousel.
The virtual master of the main turret is the whole machine's master, so each group is slave of it.

The main turret is composed by 48 of these Heating Heads and it's the heaviest and biggest group of the machine.The total weight of the main turret is around 1900 kg with an external diameter of more than 1,5 meter.

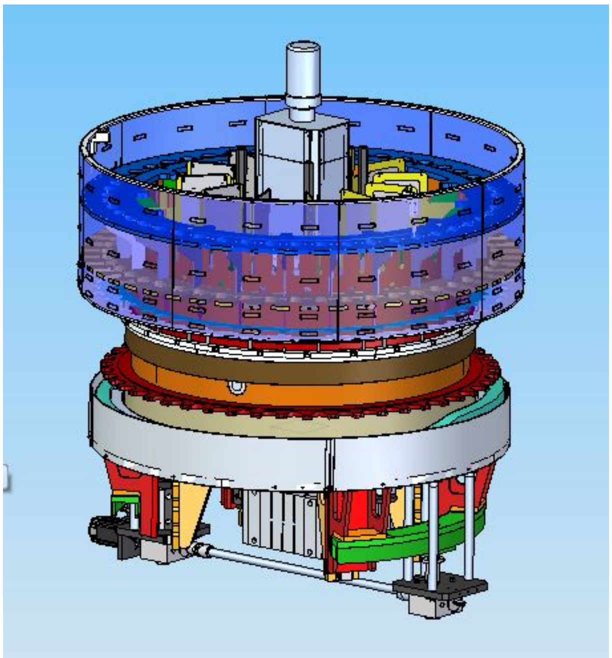

FIGURE 2.4: Cad representation of Main Turret group

During the thesis, a particular attention is payed to this group since is the highest energy consumer one.

4x Lids Transfer

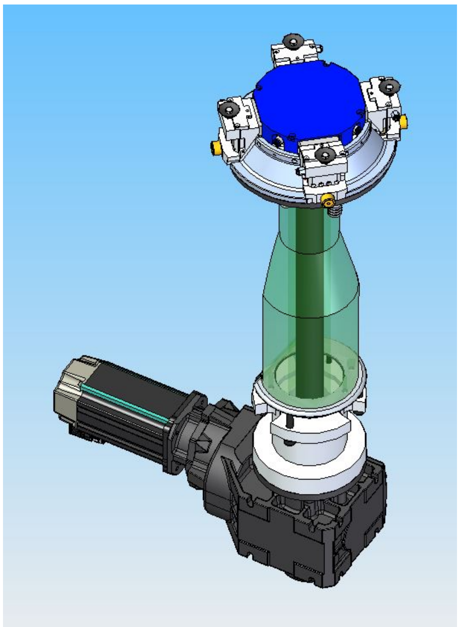

FIGURE 2.5: Cad representation of Warehouse single group

The Lids Transfer groups are 4 twins groups that have the role to grab the caps from the warehouse and position them on the Heating Heads of the Main Turret.
They are the only groups that have an intermittent motion since the Main Turret has a continuous motion and the Lids Transfer needs to be stopped when it grabs the caps.

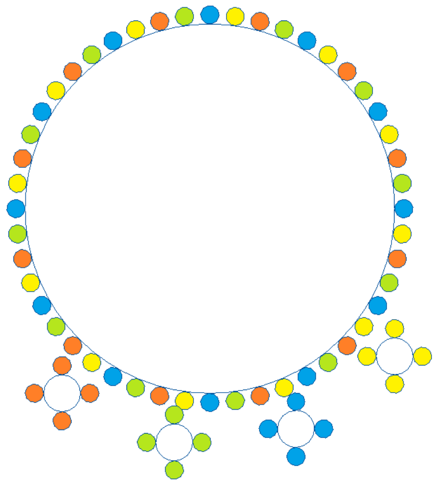

FIGURE 2.6: Distribution of caps from the warehouse groups

Since the main turret has 48 heads, each Lids Transfer feeds one head over 4. But every transfer group has 4 heads so a complete revolution is done once that each group has feed 4 heads. Consequently a complete revolution of the main turret involves 3 complete revolution of each transfer group.

4x Lids PickUp

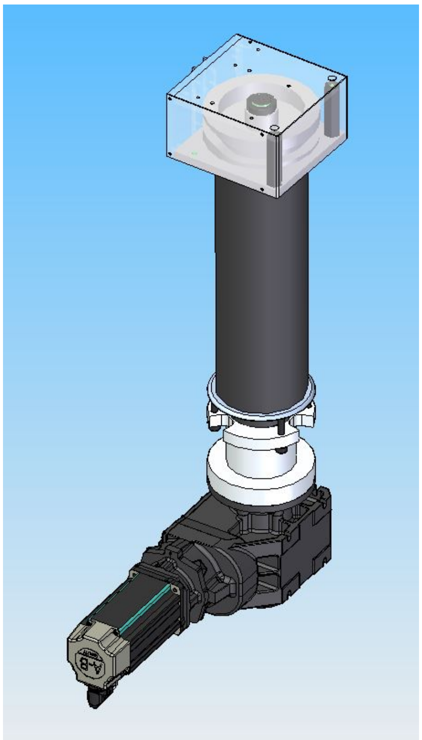

FIGURE 2.7: Cad representation of Lids PickUp group

The Lids PickUp groups are 4 twins that have the scope of move the heads of the Lids Transfer in order to catch the cans from the warehouse.
They are composed by a disc with a cam that, when rotating and correctly synchronized with the Lids transfer, performs the PickUp of the heads.

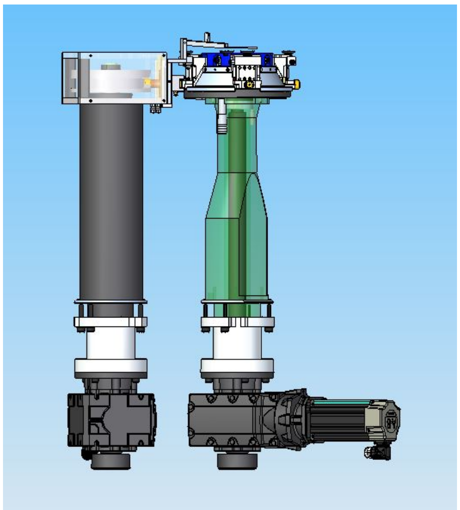

FIGURE 2.8: Lids Transfer and Lids PickUp Groups

As for the other groups, they rotate at constant speed when the whole machine is rotating constantly.

2.2 Emptying Phase

The main reason why it is necessary to recover and store energy is that, once that the main power supply shuts down, the machine needs to perform a sequence of operations before stopping. In particular the machine needs to pull out all the cans that are inside it.

During this part of the thesis, has been analyzed the worst case in which the machine could be when the grid power shuts down. All the consequent elaboration and the sizing of the K.E.R.S. are made with respect to this case.

The main phases that the machine needs to do before stop are:

- Brake until an "Emptying Velocity" is reached
- Stop the Incoming flow of products
- Wait until all the products are out of the machine
- Brake until the machine is stopped

As it will be explained in the following chapters, thanks to the construction of the Friction Model and, more in general, to the Energy Consumption Model, the worst condition in which the machine could be when the power grids shuts down is the maximum speed of operation.

This is due to the fact that all the groups are operating at the maximum velocity and that, to stop, it needs to pass the maximum amount of time.
The Stopping Strategy is designed in order to have an as nominal as possible behaviour with the goal to not stress the groups more than the necessary. The machine, infact, once that the main power supply is restored, needs to restart without a particular initialization phase or procedure.

Starting from the assumption that the machine is operating at maximum speed, the stopping phases are divided as follows:

Phase	**Productivity[$\frac{can}{h}$]**	**Time[s]**
1° Brake	55000 -> 20000	5
Emptying Phase	20000	10
2° Brake	20000 -> 0	5

Chapter 3

Physical Modeling

During this phase of the thesis has been developed the physical model of each group of the machine. After that, the model is validated through experimental data and are calculated all the flows of energy In and Out coming from the machine with simulations.
The scope of this model is infact to simulate the behaviour of the whole machine in different situations in order to understand if it is possible to recover kinetic energy and calculating the necessary amount of energy for the emptying phase.

As will be explained, all the models model's parameters come from the catalogs, mechanical CAD or from experimental data.

Since all the groups of the machine share more or less the same structure, has been decided to develop a generic model and then to tune the parameters based on the group under analysis.

The physical model of each group has been divided into 3 main models since them are present in all the groups:

- Mechanical model (inertias)
- Friction model
- Electrical model

3.1 Mechanical Model

The mechanical Model of each group has been developed by using Matlab and Simscape Tool. All the mechanical elements have been considered as rigid bodies so no elasticity of the elements has been taken into account.

After a brief analysis, it has been decided to threat all groups with a general mechanical structure composed by:

- Motor Inertia
- Reducer Inertia (Reduced to input shaft)
- Transmission Shaft Inertia
- Load Inertia

For the groups that have more elements attached to the load shaft, they have been considered as a single component identified as the Load Inertia. This Load Inertia has been calculated as the sum of all the components inertias.

All the Inertias values has been taken from the Mechanical Cad (Solid Edge) provided by the Ecocap's engineers.

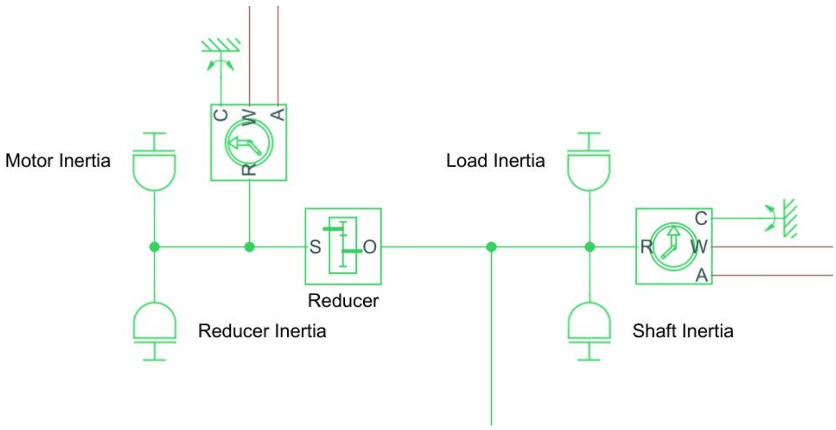

FIGURE 3.1: Mechanical model of the main sections of each group

Once that all the inertias have been defined, it has been calculated the whole inertia reduced to the motor shaft. In particular:

$$J_{tot} = J_{motor} + J_{reducer} + J_{shaft}\tau^2 + J_{load}\tau^2 \tag{3.1}$$

Where:

- J_{motor}: Motor Inertia
- $J_{reducer}$: Reducer Inertia at Input Shaft
- J_{shaft}: Shaft Inertia
- J_{load}: Sum of all load inertias
- τ: Reducer ratio

In order to simulate the movement of the group, it has been added an "Ideal Angular Velocity Source" attached to the Load Shaft. The correct velocity profile is generated by a Trajectory Generation Block, explained in the following.
At the mechanical model has been added 2 different rotary sensors in order to measure the angular velocity (in $\frac{rad}{s}$) of the 2 different shafts.
These velocities are elaborated in the other sub-models.

Inertias [Kgm^2]:

Group	Motor	Reducer	Shaft	Load	τ
Lids Transfer	0.000078	0.0000729	0.001	0.082	12.08
Lids PickUp	0.000078	0.0001513	0.001	0.021	7.82
Main Turret	0,1853	0.000644	0.177	740.103	158.81
In/Out Carousel	0.000078	0.0000146	0.002	0.3622	37.97
Screw	0.000256	0.000073	0.0006	0.0195	3

3.1.1 Trajectory Generation

For all the groups, it has been constructed a block for the generation of the velocity profile starting from the productivity parameter and ending with the velocity of the Load Shaft expressed in $\frac{rad}{s}$.
Since the productivity is expressed in can/hour, all the different groups presents different elaboration.

All the "Continuous-Motion" group's trajectory has been synchronized by using the productivity parameters and scaling it by a factor defined by each structure and size. The Lids Transfer group has been synchronized by using the cam function calculated from the given coordinates. To define the correct profile it has been used the "csapi" Matlab function calculated on a given set of points.

Once that all the groups have been synchronized, the Input variable "Productivity" has been connected to a common parameters that drives all the machine.

The phase between the groups has not been taken into account since from the energy point of view is not significant. Since the simulation is developed in a virtual environment, there will not be problem about component interferences.

3.2 Friction Model

In a first approximation the Friction model has been considered as composed by 2 different dynamic friction coefficients and a coulombian friction. In particular the two dynamic friction coefficients were considered as one referred to the elements before the speed reducer and one referred to the over ones.

Since the effects of the friction are significant only for the motor behaviour analysis, it has been decided to model the friction effects as a single friction coefficient with a Coulombian friction.

In particular, it has been considered a friction torque (seen as a resistive torque) reduced to the motor shaft.

$$C_f(t) = \beta\omega(t) + C_r \tag{3.2}$$

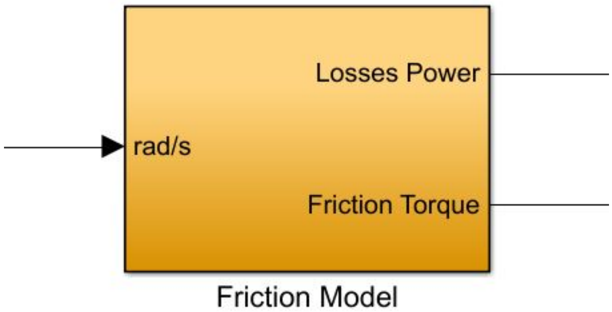

FIGURE 3.2: Friction Model's Block

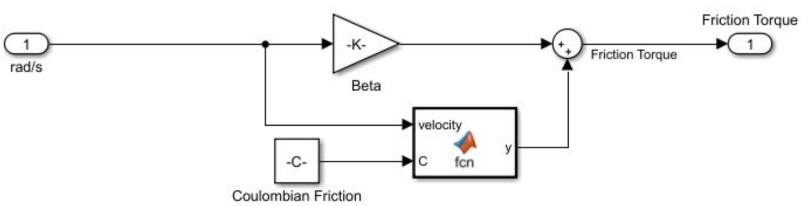

FIGURE 3.3: Friction Model's Block Inside

A function block comes necessary only for determine when the coulombian friction (the constant part of the friction torque) is active. This is done following the model:

$$C_r = \begin{cases} C_r' & \text{if } \omega(t) > T \\ 0 & \text{if } \omega(t) < T \end{cases}$$

Where T is a chosen threshold of velocity and C_r' is the value of C_r.

Otherwise, the Constant torque will be present even if the $\omega(t) = 0$. This will cause errors in the current absorption.

Then, the Friction Power losses have been calculated as:

$$\boxed{P_f = (\beta\omega + C_\mathrm{r})\omega}$$

So the Simulink implementation has been extended:

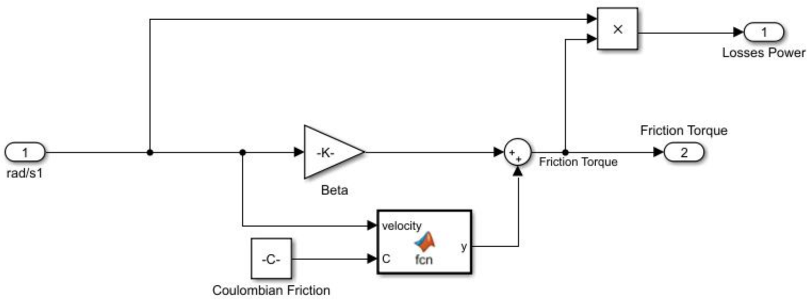

FIGURE 3.4: Friction Model's Block Extended Inside

The measure of the Friction Torque has been extracted from the block in order to be elaborated from the other blocks.

The values of the parameters β and C_r are not known and they need to be estimated with some experimental tests. This procedure is shown in the chapter "Resistive Torque Modeling".

3.3 Electrical Model

The Electrical Model of each group has been developed in order to model the Joule losses on the motor windings. In particular it has been modeled the currents coming from the accelerations/decelerations and from the Torque necessary to win the friction one.

The electrical losses on the motor's driver and other electrical components have not been modeled since they, in a first approximation, are negligible with respect to the huge losses of Joule effect and the friction.

The current that is considered as motor-current is the one that is available from the measurements of the Rockwell system. In particular it's the I_q of the Park Transform of the motor. This current is physically the one that produces Torque on the motor shaft.

Current Calculation:
In order to simulate the values of the current due to the acceleration and deceleration of the group, it has been derived the angular velocity of the motor shaft. Consequently, it has been multiplied for the total inertia reduced to the motor (3.1) to obtain the Torque due to dynamic of the mechanism.
Then, that Torque has been added to the Friction one, whose measure is coming from the Friction Model.
Once that the Total torque has been calculated, it has been divided by the Torque Constant ($\frac{Nm}{A}$) to obtain the current absorbed by the motor.

So the current can be expressed as

$$I = \frac{J_{\text{tot}}\dot{\omega} + \beta\omega + C_r}{K} \tag{3.3}$$

Then, the Joule Power Losses have been calculated as:

$$\boxed{P_e = RI^2}$$

And the Simulink representation:

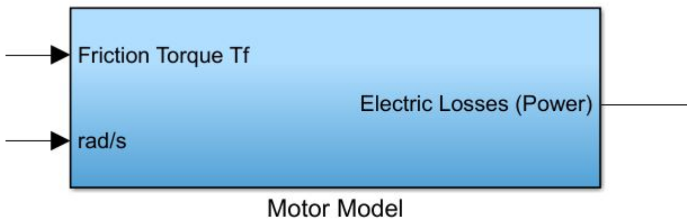

FIGURE 3.5: Electrical Model's Block

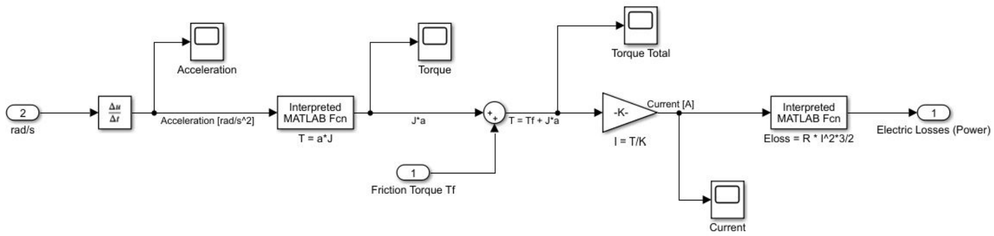

FIGURE 3.6: Electrical Model's Block Inside

All the parameters value referred to the motor comes from the Rockwell's catalogs and has not been performed any Parameter Identification Algorithm in order to calculate them.

3.4 Kinetic Energy Model

Since the scope of the project is to recover the kinetic energy from the machine, a Kinetic Energy Model must be developed in order to simulate and understand if it is possible to recover energy or if the energy consumption it to high.

This model has been realized by using the 2 angular velocities present in each group: one before the speed reducer and one over it. Then the canonical expression of the kinetic energy is used differentiating the different components for each angular velocities.
The final expression is:

$$T(t) = \frac{1}{2}J_m\omega_m(t)^2 + \frac{1}{2}J_l\omega_l(t)^2 \tag{3.4}$$

Where:

- $J_m = J_{\text{Motor}} + J_{\text{SpeedReducer}}$
- $J_l = J_{\text{Shaft}} + J_{\text{Load}}$
- $\omega_m = MotorAngularVelocity$
- $\omega_l = LoadAngularVelocity$

Then, since the final elaboration requires a power balance, this energy has been derived in order to obtain the power flows In and Out from the mechanical component.

$$\boxed{P_k = \frac{d(\frac{1}{2}J_m\omega_m(t)^2 + \frac{1}{2}J_l\omega_l(t)^2)}{dt}}$$

The final step consists in adding in the power balance only the recovered kinetic energy. This means that the power flow of kinetic energy has to be considered only when the machine is braking, so when the power flow is negative.

With some elaboration, it comes easy to have the final Kinetic Energy Model:

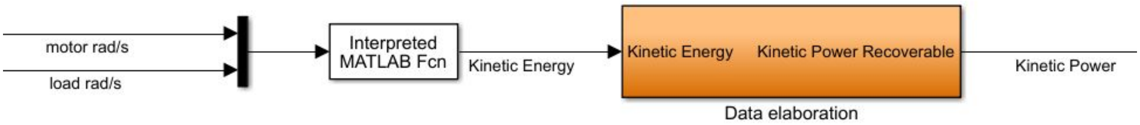

FIGURE 3.7: Kinetic Energy Model's Block

Consequently they are transformed in Power Flows by applying a derivative and then the final result is calculated by applying a Power Balance to all the flows.

Chapter 4

Resistive Torque Modeling

The problem of the energy loss is due both to the electrical effects of the motor and the friction that all the mechanical elements have in the whole machine.
This phase of the thesis involves the modeling of these resistive torques using elaboration of experimental data.

The tests performed on the machine are divided into 2 main groups of tests:

1. **Constant Speed Tests**
   The aim of these tests is to collect a sufficient number of data in order to estimate the friction parametersβ and C_r.
   These tests have been performed at constant speed since in this condition, as will be explained, there is no current related to the dynamic of the group (except for the LidsTransfer Group). It's then possible to isolate the friction torque from the dynamic one.

2. **Ramps Tests**
   The aim of this second set of tests is to validate the model of each group and adjusting the Inertias coming from the cad with the ones coming from the elaboration of data.
   A second objective of these tests is to have a first experimental estimation of the Energy Recoverable from the machine by looking at the currents behaviour.

4.1 Constant Speed Tests

The tests that have been performed consist in the data sampling of the current of each motor (directly related to the torque applied) and the position/velocity/acceleration provided by the board encoders.
Since all the groups are operating at constant speed, the current absorbed by the motor can be expressed as:

$$I = \frac{\beta\omega + C_r}{K} \tag{4.1}$$

The tests have been performed at constant speed of the machine with all the groups active and has been repeated for 4 different velocities:

- 20% of Max Speed
- 50% of Max Speed
- 80% of Max Speed
- 100% of Max Speed

Remember that the Max Speed means 55000 cans/hour.

If the assumption on the friction model expression is correct, the experimental data should show a linear (or quasi-linear) dependency of the Torque (current) with the angular velocity of the motor. In addition, this linear relation should be shifted up by an offset due to the Coulombian Friction.

Procedure:
This elaboration has been developed by collecting a sufficient amount of samples with a consequent calculation of the mean value. At this point, the mean values of the current has been placed as a function of the angular velocity of the motor expressed in $\frac{rad}{s}$ instead of the percentage of the maximum speed.
Then it has been found the line that best fits the 4 means with the Least Squared Method.
Since, as will be shown, the lines obtained fit with a very good approximation the mean values of currents, no more elaboration has been developed.
Once that the line equation has known, the angular coefficients and the Y-Axis intersection have been extrapolated and considered as β and C_r.

This data elaboration has not been developed for the LidsTransfer group since even if the machine runs to a constant speed, it will follow the cam previously defined. As will be explained, for that group has been applied a more complex identification algorithm.

All the tests have been performed for the duration of 10minutes with a sample interval of 2ms. The duration of the tests have been decided in order to obtain at least 1500 cycles of the Lids Transfer Groups at each velocity (the identification algorithm for the Lids Transfers has been applied to the same set of data). At the slowest velocity the productivity is of 11000 $\frac{can}{h}$ that corresponds to more than 1800 cycles. Then, just for simplicity, all the tests have been performed for 10 minutes.
All the data have been measured and recorded by using the Rockwell system and subsequently elaborated with Matlab.

During the thesis, these tests have been performed two times:

- Starting from "Cold" condition
- Starting from a "Steady State" condition

The set of tests performed from the "Cold" condition have been developed by recording the data as soon as the machine has been started. In this way, the data show some particular effects due to the fact that all the mechanical elements and the lubrificants involved in the kinematic chains need to reach the operating temperatures.
In particular the currents shows a transitory effect, this means that the torque applied to the cinematism decreases in time until it reaches a Steady State Value.

The results of this first set of tests have not been taken into account for the Friction Model since the friction parameters are not time invariant.

Anyway the effects are shown in the following.

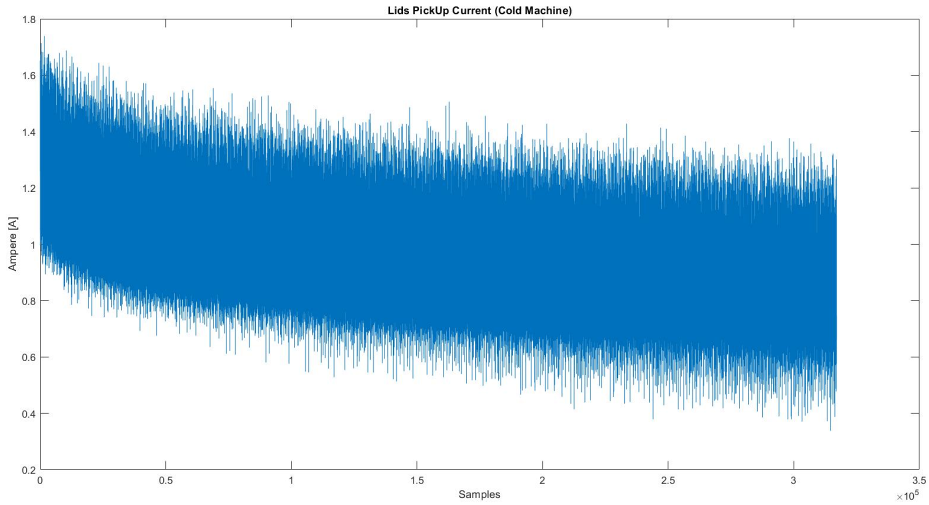

FIGURE 4.1: Current of the Lids PickUp group at V=100%

As can be seen, as the time goes on the current required from the Lids Pick Up group is lower. This because the temperature of the speed reducer's oil rise up and consequently the friction effects decrease.

The second set of tests have been performed after letting the machine running for 30minutes at maximum speed. In this way, all mechanical part and the lubrificants have reached the thermal steady state.
The data coming from these tests are the ones used for estimate the friction parameters.

4.2 Main Turret Group

The main turret group, as it has been said, is the group on which the attention is focused since it is the heaviest of the machine.

In the following, are represented the graphs of the currents during the 4 tests.
As can be seen, there is a high noise on the measurement.

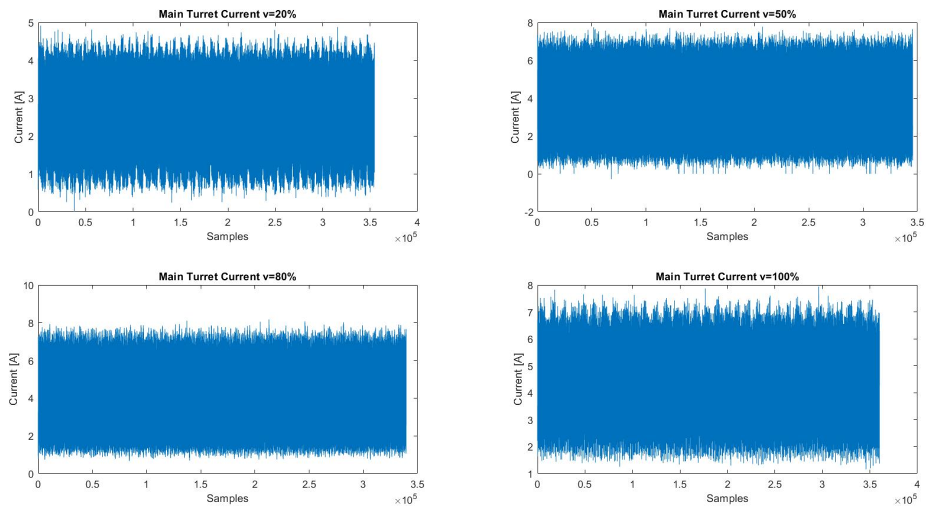

FIGURE 4.2: Currents of the Main Turret group in the 4 tests

After that the currents graphs has been analyzed, than it has been plotted a "Scatter" graph in order to analyze graphically the distribution of the samples.
As it can be seen, the variance of the samples seems not to be correlated with the velocity of the group.
Instead, it is evident an increasing behaviour of the torque with the velocity.

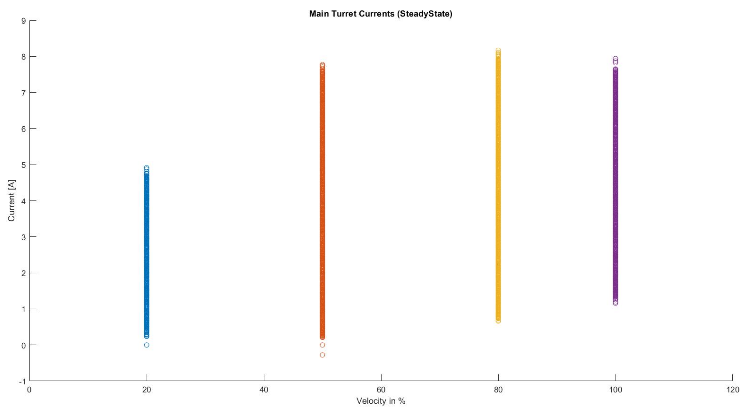

FIGURE 4.3: Currents of the Main Turret group scattered

The Last graph that has been analyzed is the Scatter one with the 4 means of the measures sampled at the 4 velocities.

The line approximates very well the behaviuour of the Friction Torque and the LS approximation can be considered as feasible.

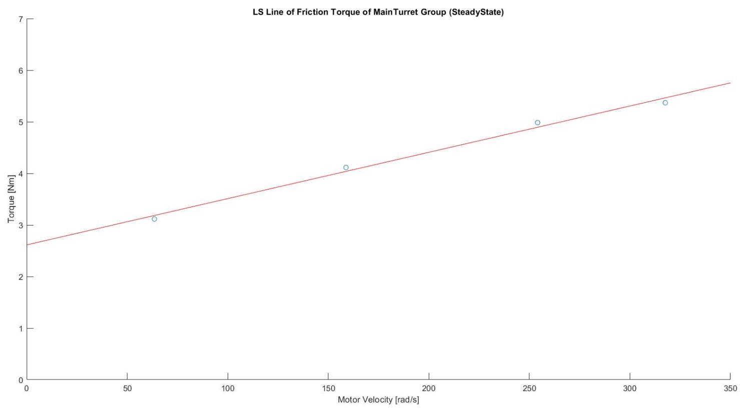

FIGURE 4.4: LS approximation of the Main Turret Samples

The experimental data shows that there is a huge energy consumption for what regarding the Main Turret Group.
This can be easily seen from the currents graphs where it's shown that the current absorbed by the motor is around few Ampers. If it's considered that there is no dynamic of the group, the energy loss due to the friction is very high.

The values of the parameters are:

- $\beta = 0.0090 \ \frac{Nm}{\frac{rad}{s}}$
- $C_r = 2.6143$ Nm

4.3 Lids PickUp Group

Even for the Lids Pick Up Group it has been analyzed the 4 sets of samples at the 4 different velocities. Also in this case, there is a huge noise on the measurements but, unlike the Main Turret Group, the values of the currents are almost always under 1 Ampere. This means that the energy consumption of the Lids Pick Up Group will be much lower than the previous one.

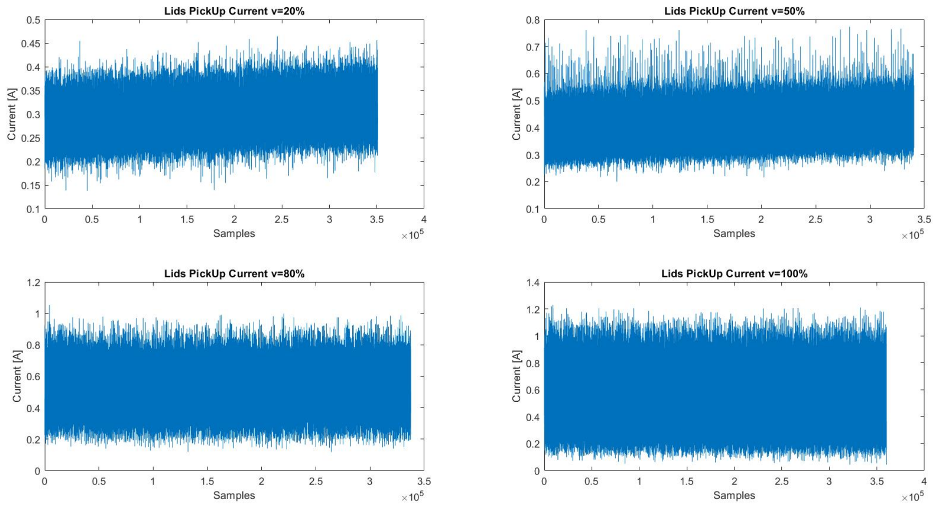

FIGURE 4.5: Currents of the Lids Transfer group in the 4 tests

For the Lids Pick Up Group, it is evident an increasing behaviour of the current with the velocity, like in the previous group. This is due to the fact that the Lids Pick Up group's velocity is a function of the productivity of the machine.

The first scatter graph shows that the variance of the samples is increasing with the velocity of the group. The relation seems to be quasi-linear.

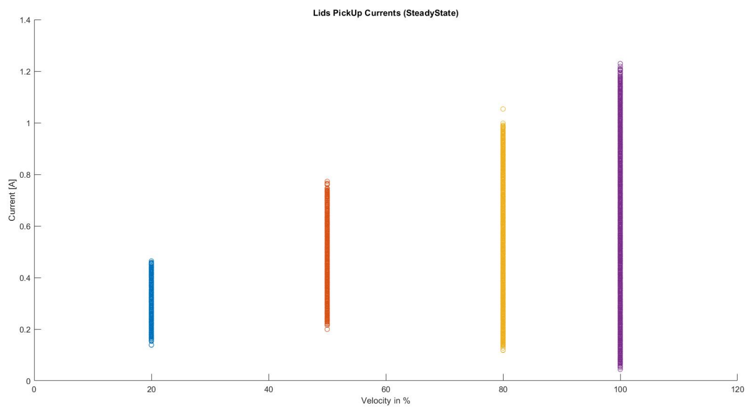

FIGURE 4.6: Data Elaboration To Isolate Recoverable Kinetic Energy

The means graph shows, even in this case, a quasi-linear relation of the mean values of the currents with the velocity of th group. So, the LS approximation of the Line can be considered as a reliable model of the Friction Torque.

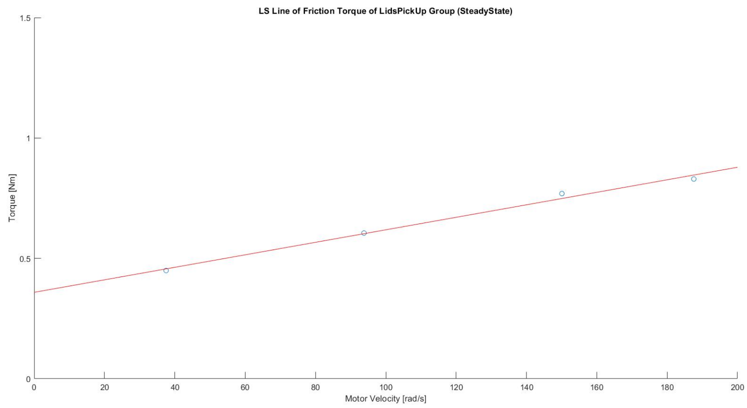

FIGURE 4.7: Data Elaboration To Isolate Recoverable Kinetic Energy

The values of the parameters are:

- $\beta = 0.0026 \ \frac{Nm}{\frac{rad}{s}}$
- $C_r = 0.3590$ Nm

4.4 Infeed/OutFeed Carousel Group

For what it regards the 2 Carousels, as previously said, the tests have been performed only on 1 group, since them are structurally twins.
As for the other groups, the plots of the currents show the presence of a noise on the measurements.

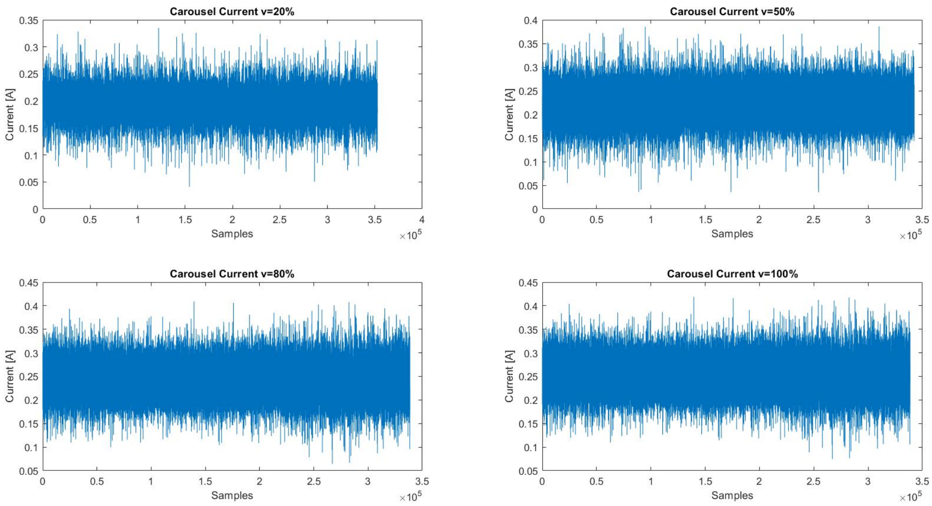

FIGURE 4.8: Data Elaboration To Isolate Recoverable Kinetic Energy

A first comparison of the Friction with the other two groups is shown by the values of the samples, that never reaches 0.5 Ampere. This means that the Carousels Friction is lower than the Lids Pick Up one, even if the dimensions of the Carousel Groups are really higher.
This is due to the fact that the Lids Pick Up Groups rotates at an higher velocity with respect to the Carousels.

The scatter graph of the samples shows that the variance is more or less the same along the different velocities, unlike the previous cases.

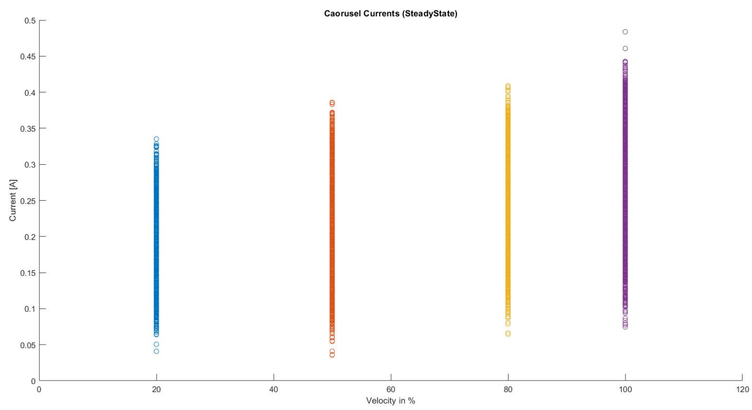

FIGURE 4.9: Data Elaboration To Isolate Recoverable Kinetic Energy

Also for this groups, the LS approximation of a linear model for the mean values is feasible.

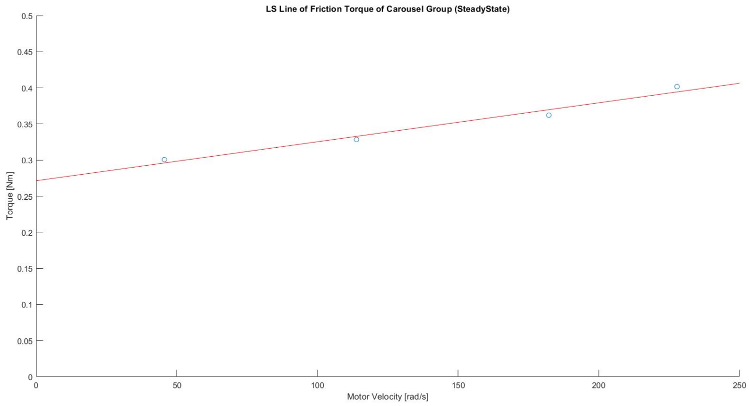

FIGURE 4.10: Data Elaboration To Isolate Recoverable Kinetic Energy

The values of the parameters are:

- $\beta = 0.00054\ \frac{Nm}{\frac{rad}{s}}$
- $C_r = 0.2714$ Nm

4.5 Infeed Screw Group

The last group analyzed with the "Constant Speed Method" is the Infeed Screw.
This group has an angular velocity higher than the previous ones since 1 revolution of the screw corresponds to 1 can step.
Due to this fact, the currents graphs shows higher currents, even higher than 1.2 Amperes at maximum velocity.
Even in this case, it is present a huge noise on the measurement.

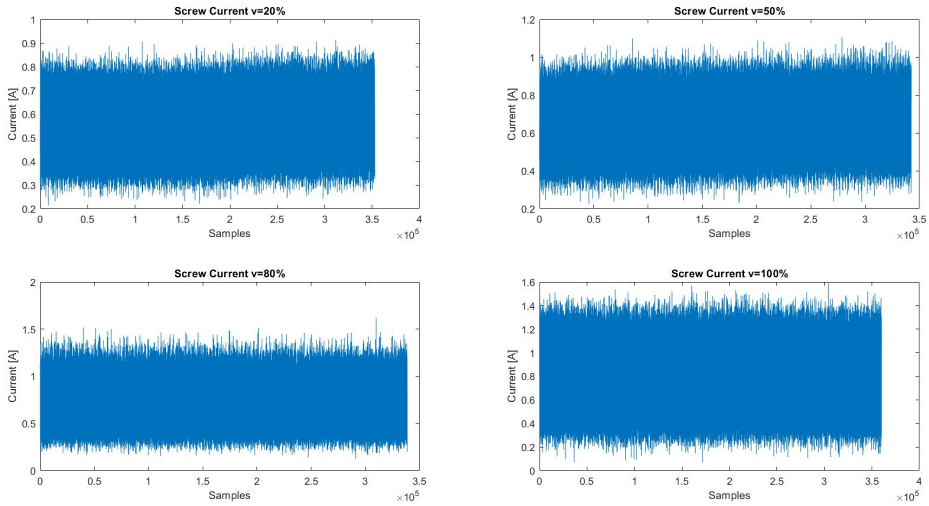

FIGURE 4.11: Data Elaboration To Isolate Recoverable Kinetic Energy

The scatter graph shows that the variance in higher in the last two tests and lower in the first two. This situation is completely different with respect to the other groups.

Unlike the previous cases, it is not so evident from this graph the linear behaviour of the currents with the velocity.

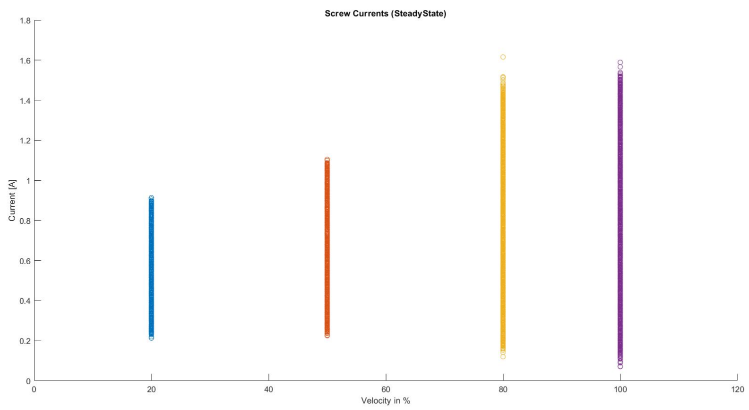

FIGURE 4.12: Data Elaboration To Isolate Recoverable Kinetic Energy

A deeper analysis is performed by the means scatter graph that reveals, unlike for what it seemed, that the linear approximation is feasible.

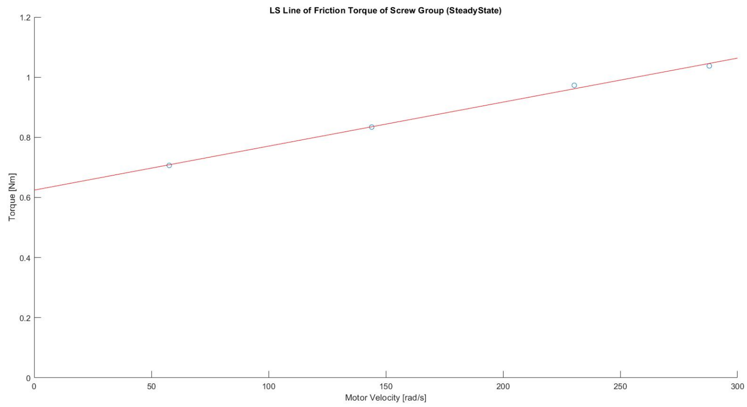

FIGURE 4.13: Data Elaboration To Isolate Recoverable Kinetic Energy

The values of the parameters are:

- $\beta = 0.0015 \ \frac{Nm}{\frac{rad}{s}}$
- $C_r = 0.6244$ Nm

4.6 Lids Transfer Group

As previously mentioned, for what it concerns the Lids Transfer Group it has been applied a Parameter Identification Algorithm in order to estimate the β and C_r. This is due to the fact that these groups follow a non-linear law of motion that is defined by a cam. As consequence, it was not possible to apply the same procedure of the other groups.

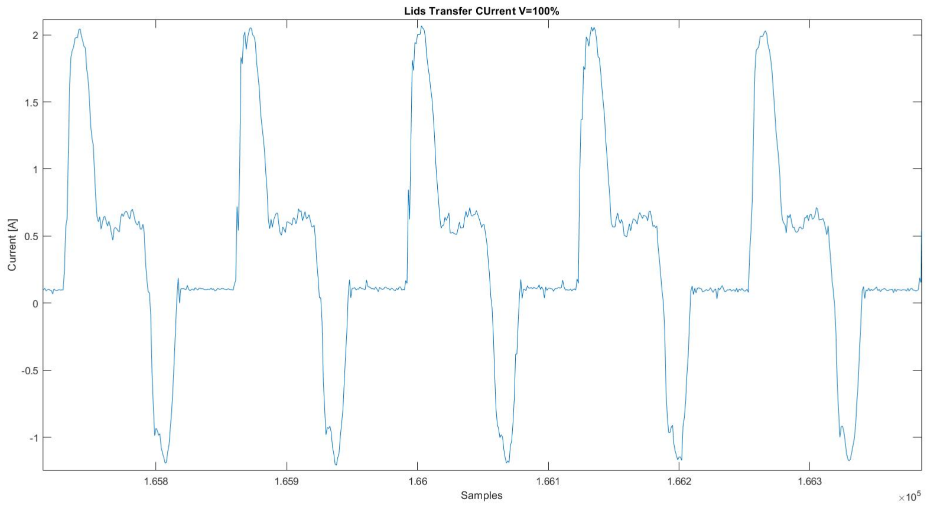

FIGURE 4.14: Current Measure of the Lids Transfer Group at V=100%

Since the Lids Transfer Group does not move at constant speed, the parameter to estimate are not just the ones related to the Friction but also the inertia of the mechanism. This is due to the fact that there is a dynamic of the group during the tests.

The parameters identification algorithm has been performed on the data sampled during the "Constant Speed Tests", so the data involves 4 sets of samples related to the 4 previously defined velocities.

4.6.1 Parameter Identification

The parameters identification algorithms need to be applied on a model of the system. In this case, it has been used the model described in the chapter "Physical Modeling":

$$T(t) = J\dot{\omega}(t) + \beta\omega(t) + C_r \tag{4.2}$$

Where:

- T is Torque applied by the motor
- J is the Group's Inertia reduced to the motor shaft
- β, C_r are the Friction Parameters
- $\dot{\omega}, \omega$ are the acceleration and velocity of the motor shaft

Without loss of generality, the model can be written in the form:

$$KI(t) = J\dot{\omega}(t) + \beta\omega(t) + C_r \tag{4.3}$$

Where:

- K is Torque constant of the motor
- I is current absorbed by the motor

The Identification Algorithm needs to be applied on a **discrete time model**, so the model described has been discretized as follows:

$$\omega(t+1) + a_1\omega(t) = b_1 I(t) + b_2 1 + e(t) \tag{4.4}$$

- **Equation Error:**
  The equation error $e(t)$ in the above equation, represents the whole errors present in the model. Since all the terms of the equation comes from measurements, them are affected by a measurement noise. In particular, it's present even on the Input.
  The solution for this problem requires a more sophisticated method in order to estimate a solution space (3 dimensions in this case, given by J,β and C_r) in which could be very difficult to find the exact solutions.
  Due to the scope of the project, has been decided to concentrate all the measurement noise into one term $e(t)$ and apply a "Canonical" Least Squares algorithm.

- C_r **Input:**
  The C_r parameter of the friction effects has been threated as an input of the model. Since it is a constant signal, it has been modeled as a constant unit input multiplied for a parameter b_2. In this way, the parameter C_r is represented by the term b_2.

This model can be applied to the different sets of data separately. Since the tests have been performed at 4 different velocities and the data related to the transitions has not been recorded, then this model can not be applied by using the 4 sets of data merged together.
The consequence is that the identification algorithm gives 4 different results for the 4 velocities.

A second possibility for what it regards the model involves the usage of the acceleration data that is available from the Rockwell system.
The model is described as:

$$a_1\dot{\omega}(t) + a_2\omega(t) = b_1 I(t) + b_2 1 + e(t) \tag{4.5}$$

In this way the model described is a **Static Model** and can be used also for the merged set of data.
Another consequence is that the coefficients a_1, a_2, b_1, b_2 are directly related to the continuous time ones, so there's no need to calculate the parameters from the poles and zeros of the transfer function.

At the end, the two possibilities for the model are:

1. **Dynamic Model:**
$$\omega(t+1) + a_1\omega(t) = b_1 I(t) + b_2 1 + e(t) \tag{4.6}$$

2. **Static Model:**
$$a_1\dot{\omega}(t) + a_2\omega(t) = b_1 I(t) + b_2 1 + e(t) \tag{4.7}$$

Thanks to the advantages just explained, the model chosen is the Static One.

Since in the described model there are 2 Inputs and 2 Outputs and all the samples are available, has been decided to further modify the model in order to have 1 Output and 3 Inputs.

In this way, the **Final Model** is:

$$\dot{\omega}(t) = \frac{b_1}{a_1}\omega(t) + \frac{b_2}{a_1}I(t) + \frac{b_3}{a_1}1 + e(t) \tag{4.8}$$

The model described is an ARX (Auto Regressive Exogenous) model, therefore it can be used a Least Squares Identification Algorithms for estimate the parameters.

At that point, it has been constructed the Hankel Matrix that is necessary to apply the Least Squares Algorithm.

$$H = \begin{bmatrix} -Y(1) & U_1(1) & U_2(1) & U_3(1) \\ -Y(2) & U_1(2) & U_2(2) & U_3(2) \\ \vdots & \vdots & \vdots & \vdots \\ -Y(N) & U_1(N) & U_2(N) & U_3(N) \end{bmatrix}$$

Where:

- $Y = \dot{\omega}$
- $U_1 = I$
- $U_2 = \omega$
- $U_3 = 1$

Since the parameters to be identified are only 3 instead of 4, the first column of the H has been deleted and converted into a H_u, otherwise the vector of parameters estimated gives [-1 0 0 0].
So the updated H_u becomes:

$$H_u = \begin{bmatrix} U_1(1) & U_2(1) & U_3(1) \\ U_1(2) & U_2(2) & U_3(2) \\ \vdots & \vdots & \vdots \\ U_1(N) & U_2(N) & U_3(N) \end{bmatrix}$$

At that point, has been applied the Least Square method:

$$\hat{\theta} = (\frac{H_u^T H_u}{N})^{-1} \frac{H_u^T Y}{N} \tag{4.9}$$

The Identification algorithm gives a vector of estimated parameters that can be described as:

$$\hat{\theta} = \begin{bmatrix} \hat{\theta}_1 \\ \hat{\theta}_2 \\ \hat{\theta}_3 \end{bmatrix} = \begin{bmatrix} \frac{b_1}{a_1} \\ \frac{b_2}{a_1} \\ \frac{b_3}{a_1} \end{bmatrix} = \begin{bmatrix} \frac{K}{J} \\ -\frac{\beta}{J} \\ -\frac{C_r}{J} \end{bmatrix}$$

At the end, the final parameters are given by:

$$J = \frac{K}{\hat{\theta}_1} \tag{4.10}$$

$$\beta = -\hat{\theta}_2 J \tag{4.11}$$

$$C_r = -\hat{\theta}_3 J \tag{4.12}$$

Numerically, it comes out that:

- $J = 0.00059584\ Kgm^2$
- $\beta = 0.0044\ \frac{Nm}{\frac{rad}{s}}$
- $C_r = 0.2797$ Nm

The results coming from the 4 different tests at the different velocities and the one considering them together are the following:

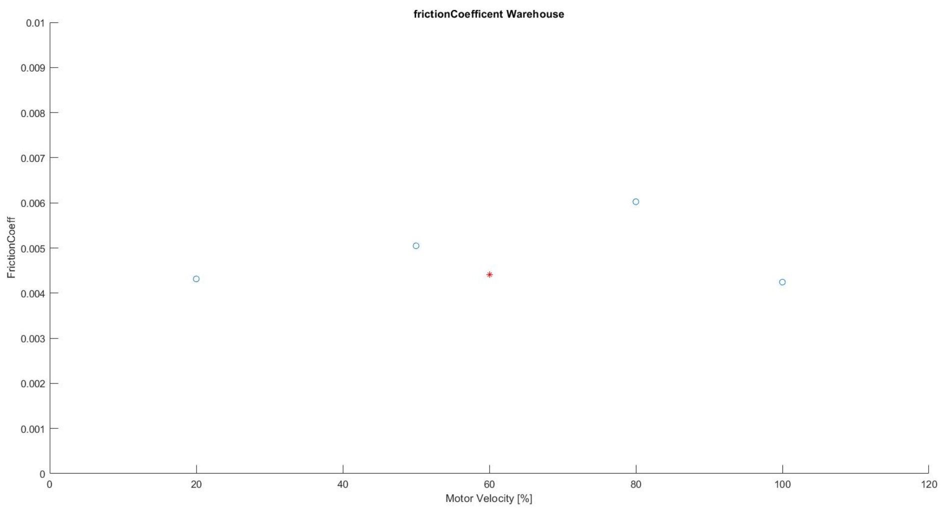

FIGURE 4.15: Comparison of the Friction Coefficients β of the 4 tests separately and together

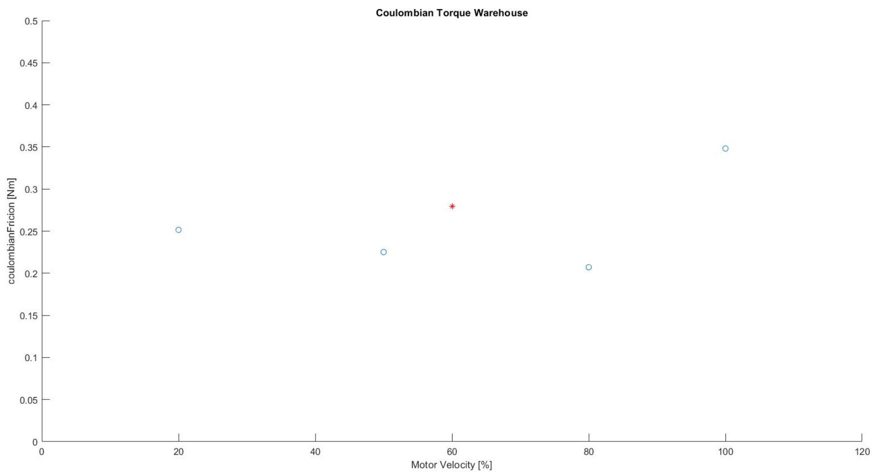

FIGURE 4.16: Comparison of the Coulombian Torques C_r of the 4 tests separately and together

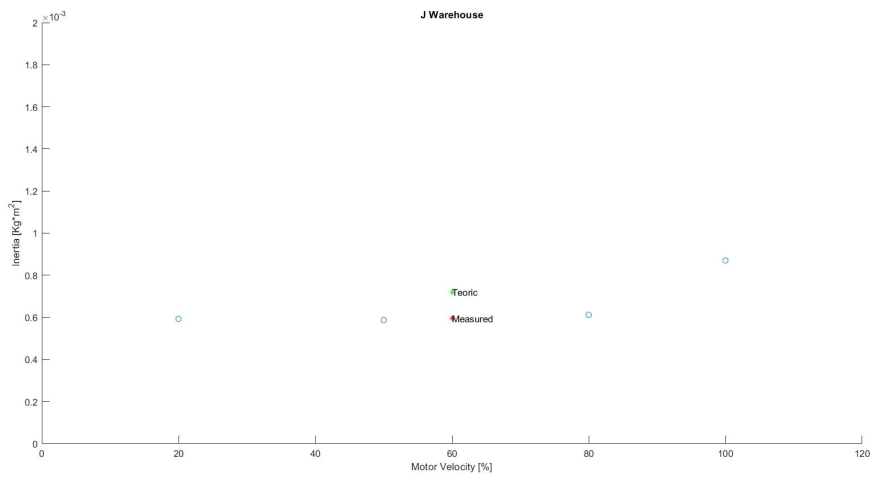

FIGURE 4.17: Comparison of the Teoric Lids Transfer Inertia and the Measured one

The result of the tests considered as one is shown at the velocity of 60%. This has been done just to compare it with the other values.
The values that have been considered for the model are the ones coming from the merge of the 4 tests, so the ones labeled as red dots in the graphs.

For what it concerns the total inertia, the value coming from the tests has been used to correct the one used for the simulations.

4.6.2 Final Results

At the end of the tests, the final results gives the following situation:

Group	C_r	β
Lids Transfer	0.2797	0.0044
Lids PickUp	0.3590	0.0026
Main Turret	2.6143	0.0090
In/Out Carousel	0.2714	0.00054
Screw	0.6244	0.0015

The following images represents the comparison between all the groups of the friction parameters β and C_r.
In order to represent graphically the camparison, it has been associated a number to each group:

1. Lids Transfer Group
2. Carousel Group
3. Main Turret Group
4. Screw Group
5. Lids Pick Up Group

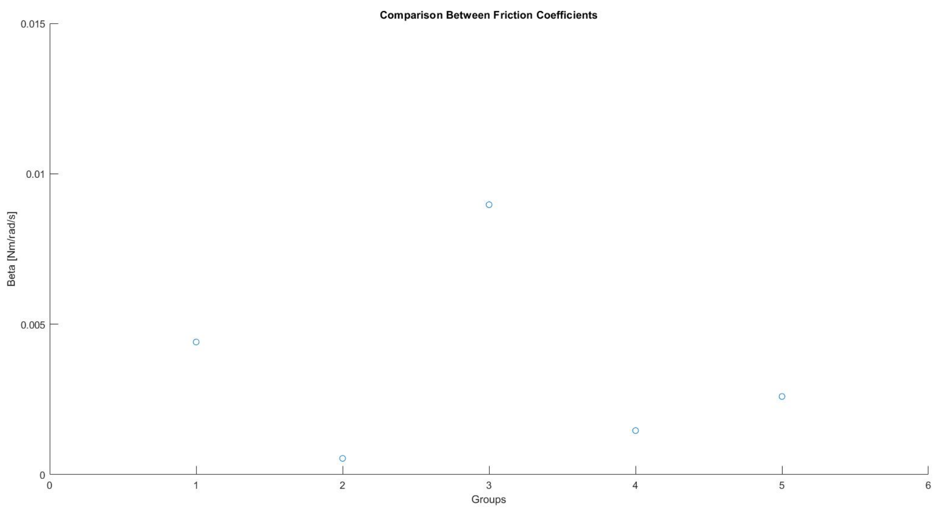

FIGURE 4.18: Comparison of the Friction Coefficients β

As shown, the Main Turret Group has the highest friction coefficient. This is due to the fact that the motor rotates at high velocity in order to have the necessary Torque at the load shaft. Since the Speed reducer has an oil lubrication, then the dynamic friction coefficient will be larger for this group.
Even the Lids Transfer Group shows a similar behaviour due to the high dynamic of the cam.

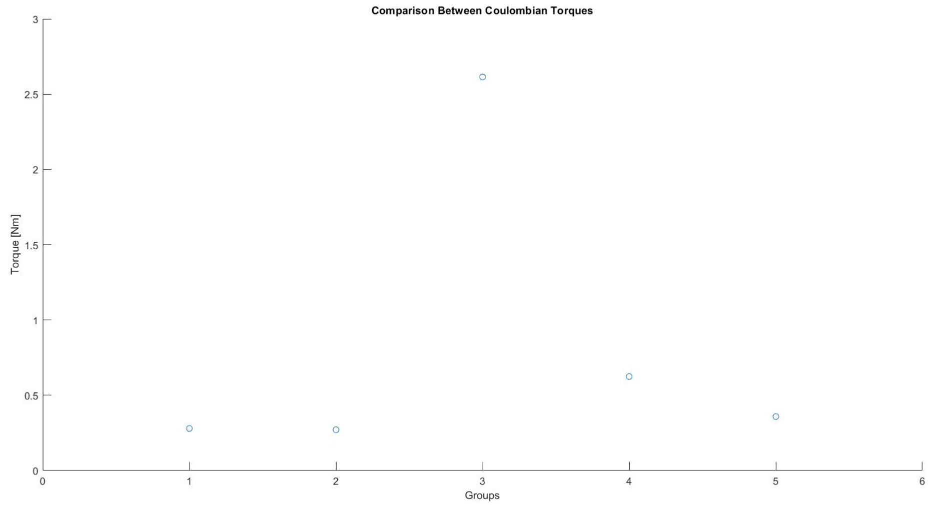

FIGURE 4.19: Comparison of the Friction Coefficients C_r

Even for what it regards the Coulombian Friction the Main Turret Group has the highest value. In this case, the reason is due to the huge mass of the Turret that is near 2 tons. The Coulombian force infact can be modeled as a coefficient times a normal force with respect to the contact surface. In this case, the normal force is related to the weight of the Turret and the Coulombian force is converted into a Torque.

Unlike for the dynamic friction coefficient, for the Coulombian Torque the others groups show a huge difference of the values.

4.7 Ramp Tests

The second set of tests have been performed in order to validate the models and to have a first experimental feedback on the possibility to recover kinetic energy and on which group are able to do it.

These tests are performed by letting the machine follow a series of acceleration/deceleration ramps. These ramps are defined starting from stopped, arriving to the max productivity and then brake to stop again the machine.

In this way all the groups are affected by a dynamic and it's possible to check if the currents (related to the torques) become negative. Remember that it's possible to recover energy only if the $T(t)\omega(t) < 0$.
By using the Friction Values coming from the previous tests it's also possible to check if the inertia values set in the model are corrects and, if necessary, update them.

The ramp tests have been performed by recording Currents, Angular Velocity and Angular Acceleration of each group by using the Rockwell System.
The sequence of ramps used for the test is:

N.	Ramp Type	Time[s]
1	Acceleration	15
	Deceleration	15
2	Acceleration	20
	Deceleration	20
3	Acceleration	30
	Deceleration	30
4	Acceleration	10
	Deceleration	10
5	Acceleration	5
	Deceleration	5
6	Acceleration	3
	Deceleration	3
7	Acceleration	3
	Deceleration	3Emg
8	Acceleration	3
	Deceleration	3Emg

The last 2 deceleration phase identified as "3Emg" define the Emergency stop that is performed by the machine in 3 seconds. These two stops are performed by physically press the emergency button of the machine.
As will be shown, the consequences due to this type of stop are quite different from the others.
The previous 3seconds stop is instead set as normal stop of the machine.

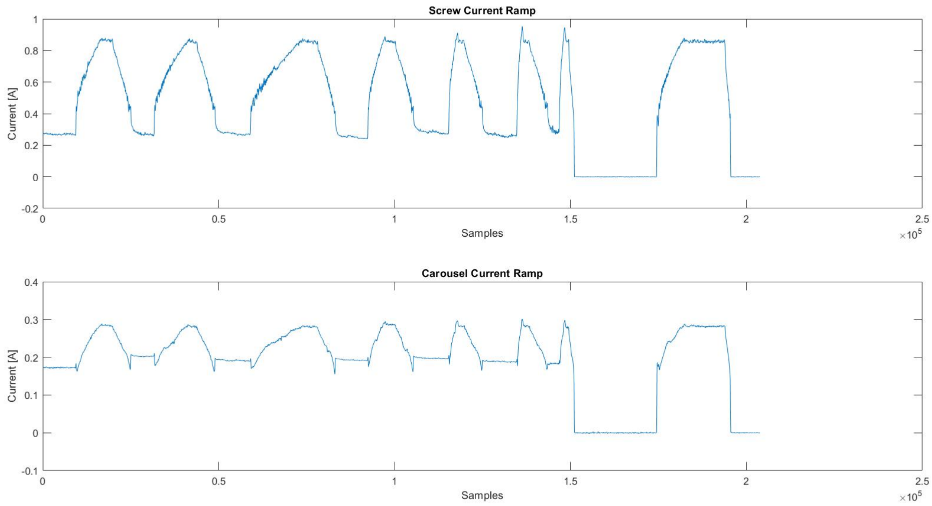

FIGURE 4.20: Ramps Currents of Screw and Carousel Groups

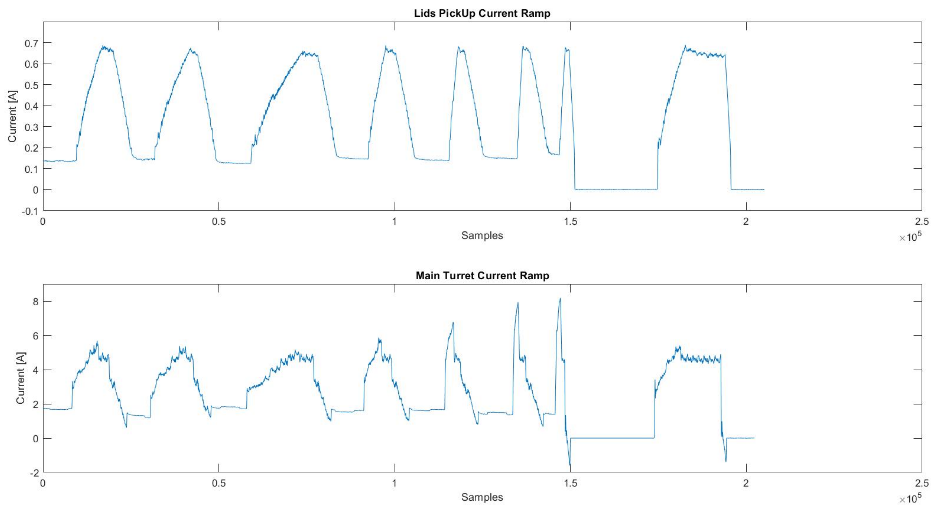

FIGURE 4.21: Ramps Currents of PickUp and Main Turret Groups

The figures above show the currents data during the ramp tests.
The currents, during the stops, do not fall to zero because the motors, even if they are stopped, are "on torque" and needs to compensate some vibrating effects due to the non-optimal gains of the controller.
Instead, after the emergency stop, the power supply is physically shut down, so the currents go exactly to zero.

Results:
The results shows that is not possible to recover energy at all from the continuous-motion groups. It's evident that there's no group that gives a negative current during the brakes, except the Main Turret for some instants during the emergency brakes.

The most unexpected result comes from the Main Turret group: as said at the beginning of the thesis, this group is the one on which is focused the attention during the analysis. This is because, in a first assumption, the huge mass of the components suggests that the kinetic energy stored in the Turret is higher than the energy lost during the brakes, with a consequent recovery of a lot of energy.
These results show the opposite: in order to stop the group, it's necessary to apply torque to follow the ramp reference, even if it's fast. This means that the friction effects are very high in the machine and all the energy is lost in them.

It's necessary to specify that the small amount of energy recovered during the emergency brakes cannot be taken in care since this type of stop will not be performed at nominal conditions.

By using the data of these ramp tests, it has been calculated the real inertias of these groups in order to correct the models. The following table shows the Inertias reduced to the motor shaft.

Inertias:

Group	**Teoric**[Kgm^2]	**Identified**[Kgm^2]
Lids Transfer	0.00072	0.00059
Lids PickUp	0.00059	0.00041
Main Turret	0.037	0.048
In/Out Carousel	0.00035	0.00026
Screw	0.0025	0.0011

The correction has been applied to the Matlab models in order to have the most reliable representation of the system.

Consequences:
The first consequence of this tests is that the energy recovering needs to be performed only through the Lids Transfer groups. Thanks to their high dynamic infact, they are the only ones able to recover kinetic energy.

Another consequence is also on the control of the Kers System: as will be shown in the System Control section, the first idea to control the Kers system was to find a "sufficient high" velocity of the machine at which the kers system could be maintained at a zero or low amount of energy stored. This because, since the energy is though as "Stored" as kinetic form inside the machine, the Kers system needs to be activated only when is performed the first phase of the Emptying Phase where the machine is braked.
After this test, this control approach has been abandoned.

Chapter 5

System Realization

In this part of the Thesis, different methods and technologies have been analyzed to realize the physically the needed system.

5.1 Battery Approach

The first idea of a system that can store the Kinetic Energy Recovered has been a Battery. Since the Kinetic Energy coming back from the Lids Transfer Group is transformed from the Mechanical Domain into the Electric Domain by the motor, the first Idea of a component that can realize the needed system was something that can accumulate energy electrically.
In a common automatic machine structure, all the drivers usually have a capacitance and a resistor built-in to accumulate or dissipate the coming-back energy. In this way, the total energy consumption of the automatic machine will be less than the nominal one since the recovered energy can be reused.
This process is performed through the DC-Bus shared between all the drivers. Since the drivers are powered from the DC-Bus, all the recovered energy is available for all the drivers in any moment.

In this particular case, the situation is quite different because the aim is to control the flow of energy both in the recovery phase and in the reutilization phase. In particular, the scope is to store and accumulate the necessary amount of energy and to maintain it until it is necessary.

Since the component needed has to be applied on the DC-Bus, it must work in DC-Current.
Moreover, the control of the stored energy depends on the measure of some physical variables of the other groups, meaning that the device must be compatible with the Rockwell's operating system.

Unfortunately, it does not exists any device available on the market that can satisfy these requirements.

5.2 Flywheel Approach

The key idea that makes it possible to realize the needed system is that the stored energy has no necessity to be in the electrical domain. Once that the device allows the control of the flux of energy, that energy can be stored in any form.

Following this idea, the chosen system is a simple flywheel controlled by a Rockwell motor and driver. In this way, all the controls that the Rockwell's system expect for the motors are available.
As a consequence, during the nominal behaviour the kinetic energy of the machine mechanisms is transformed into electrical energy when they brake. Through the DC-Bus the electrical energy recovered is injected into the KERS System and then it is again transformed into kinetic energy of the flywheel.

Once that the power grid shuts down, the flywheel will be properly braked in order to provide an emergency power supply for the DC-Bus. By using this emergency power supply, the machine can perform the Emptying Phase previously described.

There are a lot of pro and cons by using a mechanical system to store energy:

- With a flywheel, the electric energy is converted into the mechanical one and viceversa. As a consequence, there will be more components through which the energy must flow, increasing the losses.
- The mechanical systems allows a better control due to the available tools and technology built in the drivers of the motors.
- By using a flywheel approach, the changes needed for the machine are minimals since it is needed just to add a driver to the DC-Bus.
- The installation of a Kers system requires less resources from Ecocap's. This is because the installation of a UPS System is carried by producer's engineers and not by the Ecocap's ones. In addition, the UPS system, once bought, is delivered directly to the costumer instead of the Ecocap's headquarter.
- The costs are in favour of a Kers system. As a matter of fact, even before starting to develop the project it can be assumed that the costs of a mechanical solution are lower than the ones of an UPS. This is because the cost of one driver and one motor with the necessary components to work is cheaper than the sophisticated battery involved in a UPS System.

Since the advantages of a mechanical solution are several, it has been decided to develop this type of system for the machine.

5.2.1 Flywheel Sizing

The sizing of the flywheel has been one of the most important and complex phase of the system's development. This is due to the fact that the size of the disc needs to balance the dimensions with the angular speed of rotation. In addition, the size and the shape of the disc are very significant for the cost of realization that is an important parameter.
From the calculation point of view, the problem is very nested and with a lot of variables: the size of the flywheel needs to be balanced with its velocity, but the velocity defines also the size of the motor, which in turn defines also the Torques parameters that are function of flywheel's size. In order to approach this multi-variable problem, it has been decided to impose some constraints and then develop the system based on them. At the end, simulations show if the constraints are respected or not.

The procedure has been performed following several steps explained in the following.

Emptying Phase Energy Calculation:
The firs step performed in order to size the flywheel has been the understanding of the total amount of energy that is necessary for the machine to perform the emptying phase.
Since the flywheel needs to provide the amount of energy to empty the machine, this parameter is a fundamental one to start the development.

The calculation of such needed energy has been performed by using simulations of the whole machine set in order to do the operations described in the Introduction section.

The machine has been set with the correct friction parameters found after the tests.

The model has been completed with an additional block that simulates the productivity profile during the emptying phase. This block, uses a combination of lines that determines the value of the machine productivity as a function of time.

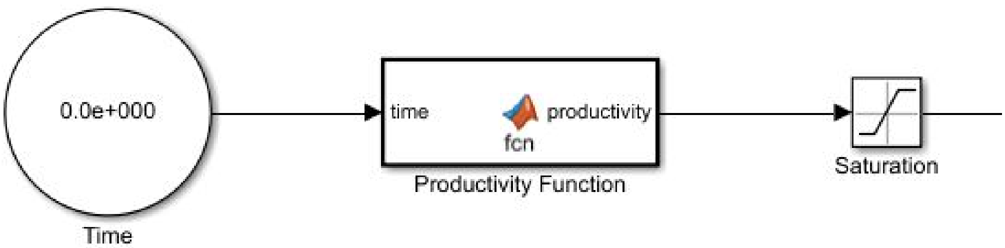

FIGURE 5.1: Emptying Phase Profile Generation

It has been added a saturation in order to maintain the productivity to zero after that the emptying phase is terminated. Otherwise, thanks to the definition of the productivity lines, it would go negative.

The lines defined are:

$$P = \begin{cases} -7000t + 55000 & \text{if } t < 5 \\ 20000 & \text{if } 5 \leq t < 15 \\ -4000t + 80000 & \text{if } 15 \leq t < 20 \end{cases}$$

The energy consumption has been calculated by adding all the power consumption of each group and then integrating it.

Final result:

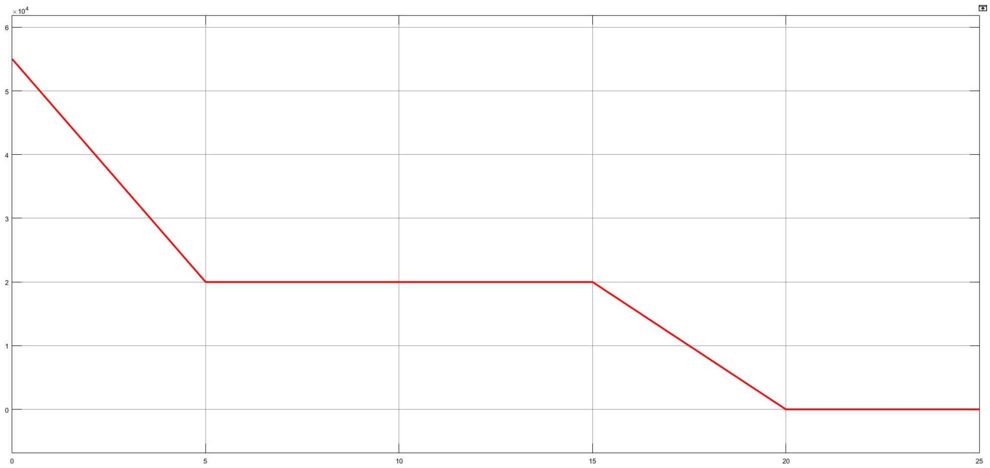

FIGURE 5.2: Matlab Simulink Representation of the Productivity in time

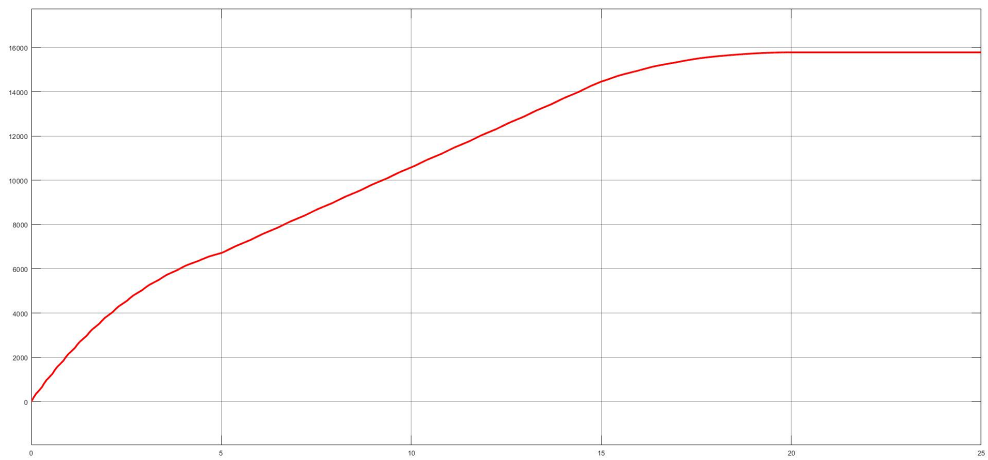

FIGURE 5.3: Energy consumption of the machine during the Emptying Phase

As shown, the total energy used to perform the emptying phase is about 16KJ. This value has been taken as reference for the following phases.

In the first phase of the brake it can be seen a small ripple of the energy profile, due to the fact that the 4 Lids Transfer Groups are recovering energy, so we have a Back-Flow of mechanical power. This effect is less evident as the simulation goes on because the dynamic of these groups will decrease in function of the productivity.

Motor Choice:
The second step performed is the choice of the motor.
To perform this phase, some assumptions have been taken, which will be better analyzed in the System Project section.

The key assumption is that the Kers system must not have a speed reducer in between the motor and the Flywheel shaft. In this way, the range of angular velocity of the flywheel is the same of the motor one. The choice of the motor is, from now on, strictly related to the size of the flywheel.

The parameters related to the motor torque have not been considered in this phase since the type of control associated to the motor involves the fluxes of energy instead of a precise law of motion. It is not possible at that point to calculate the Max and the RMS Torques in the two different operation phases of the Kers System. Furthermore, it can be easily understood that, in the energy accumulation phase, the Torque needed when the Kers starts from stationary condition would tend to infinity, so it is necessary a saturation in the control. This problem will be analyzed in the System Control section.

The motor has been chosen between the ones that the Ecocap's had already bought. In particular, the choice has been narrowed down between the ones that have an operating velocity that include the range 1500-2000 rpm. This is because this range of velocity has been voted as the optimal one for the maximum speed of a mechanical flywheel, especially for the High-Load bearings.

The chosen motor is identified as:

Allen-Bradley VPL-B1303F-PJ12AA

Main Characteristics:

- Voltage Class:...............................400V
- Rated Speed:................................4000rpm
- Continuous Torque(RMS):.........8.80Nm
- Max Torque:.................................18Nm
- Torque Constant:.........................1.33 $\frac{Nm}{A}$
- Series Type:...................................Low Inertia

Flywheel Sizing:
The last step performed has been the sizing of the physical flywheel.
This phase requires to close the loop of calculations by using all the constraints just set.

Such constraints are:

- **Angular Velocity of the Flywheel:** ....1600rpm (bond coming from bearings)
- **Total amount of energy needed:** 16KJ
- **Max Torque:** 20.8Nm
- **RMS limit Torque:** 8.80Nm

In order to calculate the necessary Inertia that the flywheel needs to have, it has been used the Kinetic Energy expression and put it equal to the necessary amount of energy (Called E).

$$\frac{1}{2}J\omega^2 = E \tag{5.1}$$

From which:

$$\frac{1}{2}J(1600 * \frac{2\pi}{60})^2 = 16 * 10^3 \tag{5.2}$$

So, the final result is given by:

$$J = \frac{2 * 16 * 10^3}{(1600 * \frac{2\pi}{60})^2} = 1.14Kgm^2 \tag{5.3}$$

At the end, in order to design a simple-realization component and have a margin of energy, the used flywheel Inertia is:

$$J = 1.65Kgm^2 \tag{5.4}$$
$$E = 23,160KJ \tag{5.5}$$

The final size of the flywheel allows to have a security margin of the energy stored.

Torque verification:
The final verification has been done by simulations and by checking the torque that the Kers System requires during the braking phase. In particular, it has been controlled the Torque of the Kers by checking the time varying velocity (starting from 1600rpm) in order to inject on the DC-Bus the correct amount of energy.
The control part has been analyzed in the detail in the System Control Section.

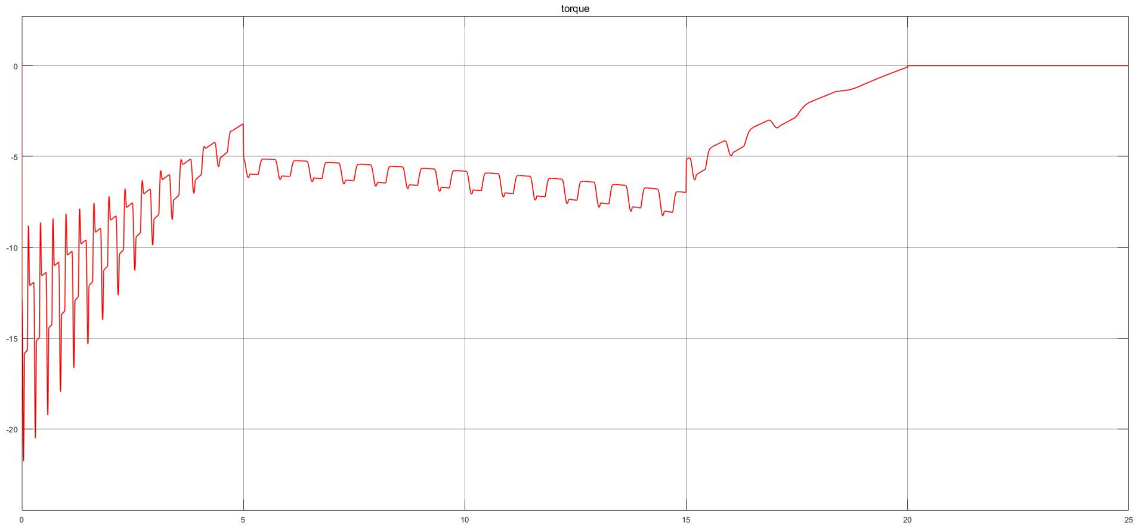

FIGURE 5.4: Simulation of the Kers Torque during the Brake phase

In the graph it can be seen the shape of the current absorbed by the 4 Lids Transfer Groups since they have a direct correlation with the torque required to the Kers. As the simulation goes on, this effect decreases, like what has been shown for the energy consumption.

The first part of the Graph shows that the Torque required is over 21 Nm, but just for some milliseconds. Therefore, the limit imposed by the max Torque is not exceeded. In addition, for what it regards the RMS Torque it can be seen that the torque is continuously over 9Nm only for 2.5 seconds. Since the limit is imposed by thermal dissipation, this overload can been accepted.
In the central part of the simulation the Torque increases because, at a constant flow of energy required by the machine, the velocity of the Kers is decreasing so the Torque needs to increase.

For what it concerns the Energy accumulation phase, it has not been performed a torque verification since in that phase it has not particular constraints: in the energy utilization case, the Torque has to follow a precise reference otherwise the machine has not the necessary energy to work. In the energy accumulation phase, there are no particular consequences if the torque imposed (combined with the velocity) does not respect the energy balance.
Furthermore, in that case, at low velocity of the Kers, the Torque required will tend to infinity, thanks to the product $T\omega$ so a saturation is also necessary. The only consequence that it can have is that the Kers "charges" itself slower, but the machine is not affected by that.

5.2.2 System Project

Since the scope is to store and maintain the energy, the mechanism has been designed in order to have less losses as possible.
The speed reducers have lubricant oil inside so the power losses are not negligible. Furthermore, it is not a strictly necessary component so it has been decided to design a mechanism without the speed reducer, as previously said.

The Final System is composed by:

- Flywheel
- Shaft
- Shrink
- Mechanical Joint
- Support frame

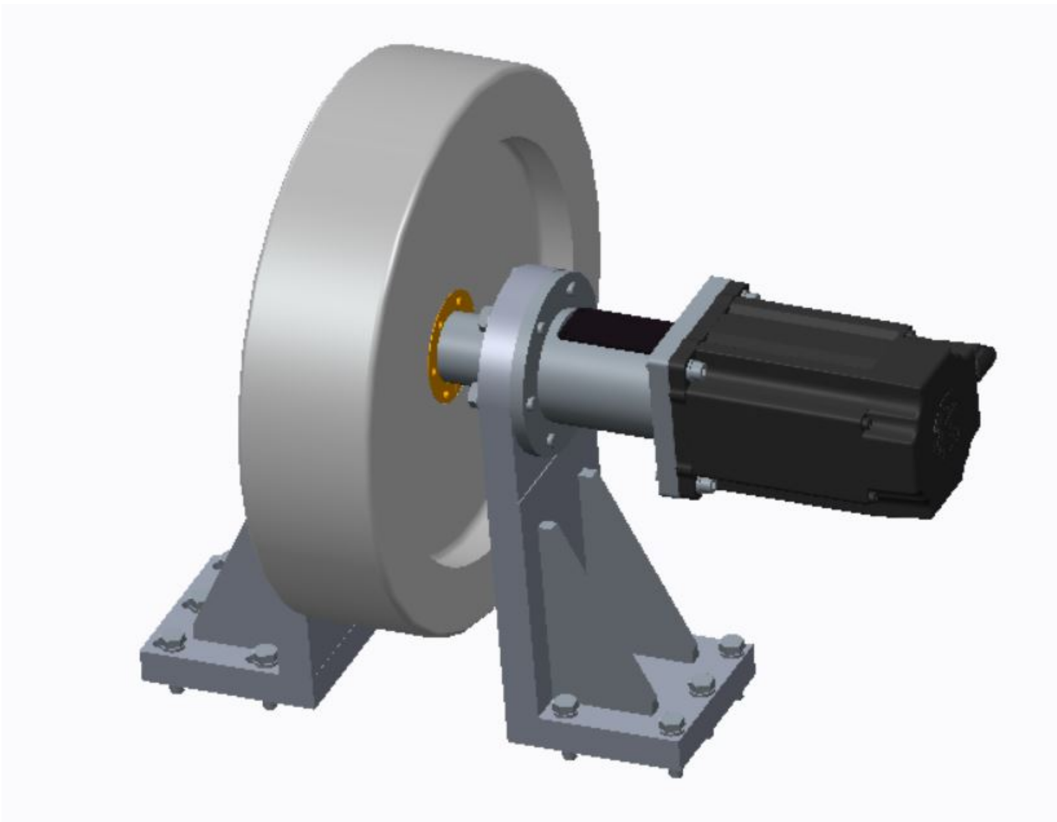

FIGURE 5.5: CAD Representation of the Kers System

The Flywheel is attached to a shaft by a Shrink and then the shaft is connected to the Motor's one by a flexible Joint. The bearings are bonded by Seeger rings and shaft/frame mechanical feedbacks.

Costs:

Component	Cost [€]
Flywheel	365
Support Bracked	190
Support Bracked Perfored	190
Shaft	100
Motor Flange	265
Motor	720
Joint	95
Shrink	10
TOTAL	**1935**

The above table does not take into account the costs of the carpentry components as screws, washers and bearings. Such components affect the costs of the system in a negligible way so the estimation can be considered a reliable one.

As it will be further explained in the Conclusion section, this cost estimation is much lower than the actually used UPS system's cost.
The used system is infact about 3 times more expansive than the Kers one.

Change on the machine:
The Ecocap's CSS648 needs some modification in order to allow the installation of the Kers System:

- **Electric Architecture:**
  In order to apply this Kers System to the Ecocap's CSS648 machine it is necessary to change the electric architecture of the drivers since they are divided into 2 different DC-Buses: a smaller one for the Lids Transfer and Pick Up groups and the bigger one for the rest of the machine.
  If the 2 Buses have no way to communicate each other, there is no possibility to provide the Kinetic Energy Recovered to the machine's motors.

  Another solution to this problem could be to apply the Kers System on the bigger DC-Bus and control it by using the energy coming from the grid. In this way the biggest part of the machine could have an emergency power supply but the solution is no longer Green. Furthermore, when a blackout occurs, the Lids Transfer Groups need to be stopped in a safe position with no interferences with the main turret.

- The other modification that is needed is the adoption of a small UPS unit in order to provide a power supply for all the electronic components of the machine(as the PLC, Hmi ecc..) that are not connected on the DC-Bus.

Chapter 6

System Control

The system control phase involves the development of an efficient control strategy for the Kers System. Since the group has been developed with a commercial drive, the control takes into account the available measurement and control algorithms present in the available system.

The control of the Kers has been divided into 2 main phases:

- **Energy Recovery Phase**
- **Energy Utilization Phase**

6.1 Energy Recovery Phase

Since the Kers system needs to accumulate exactly the amount of energy the comes back from the Lids Transfer Groups, the energy recovery phase is a crucial part of the project.
If the control does not work properly, 2 different situations can occur:

- **The Energy coming back is not injected at all in the Kers:**
  In this way, part of the kinetic energy recovered will be directed on the DC-Bus of the machine. As a consequence, that energy will be stored at the moment into the built-in Capacitance of the drivers.
  That energy is not controllable, so it will be available in any moment for the whole machine groups.
  The consequence is that the Kers needs a bigger amount of time in order to accumulate the necessary amount of energy.

- **The Kers is controlled with more energy than the necessary:**
  In this way, the energy that flows into the Kers is greater than the one recovered from the Lids Transfer Groups. As a consequence, it will occur that there is a flux of energy that is absorbed from the grid power supply, since the Lids Transfers Groups are the only ones able to recover energy.
  This situation will cause a reduction of the necessary amount of time for the kers to store the energy but the solution is not yet as green as desired.

6.1.1 Electrical Approach

The first approach analyzed for the Kers control during the energy accumulation phase was an Electrical Approach. The idea was to use the measure of the current absorbed by the motor combined with the voltage applied in order to estimate the flux of electrical energy.
It has to be taken into account that the current measured is the I_q of the Park's Transform, that is the one that generates torque.

Once that the flux of energy has been estimated, the idea was to apply a control to the Kers Group in order to inject the same amount of energy just recovered by using the same approach.
In particular, the control has to be applied to the current to have equal fluxes of energy.

This procedure requires both the measure of the currents and the measures of the applied voltages to the motors.

Unfortunately the measure of the voltage applied to the motor is not available since it is not so easy at it seems. The voltage is not related to the DC-Bus one because the motors need three sinusoidal waveforms properly applied.

Due to these problems, this approach has been abandoned in favor of a mechanical approach.

6.1.2 Mechanical Approach

The Mechanical approach uses the same idea of the electrical one. The scope is to estimate the amount of mechanical energy that is recovered from the Lids Transfer Groups and control the mechanical variables of the Kers one to inject the correct amount of energy.

By using a mechanical approach the variables used are the Torque T and the angular velocity ω.

Procedure:
During the energy recovery phase, the angular velocity ω and the Torque T of the Lids Transfer Groups are continuously checked. The mechanical power In/Out coming from such groups is given by the product of the two measures.

$$P_{mechanical} = T\omega \tag{6.1}$$

Defined a rotational direction as reference, the sign of the Mechanical Power shows if the Lids Transfer Groups are absorbing or returning energy.
Actually, since the rotation can be only in one direction, we can obtain the same information by looking at the sign of the current.

If the current shows that the groups are returning energy, then the Kers is controlled by using the information of the mechanical power returned.
The control applied to the flywheel is a Torque control where the profile of the reference is obtained by dividing the value of the incoming power by the actual angular velocity of the Kers.
After that, a saturation of the reference is applied because at low velocities the needed torque could be very high.

Final control algorithm:

1. $$P_m = \begin{cases} 0 & \text{if } I_1, I_2, I_3, I_4 > 0 \\ T_1\omega_1 + T_2\omega_2 + T_3\omega_3 + T_4\omega_4 & \text{if } I_1, I_2, I_3, I_4 < 0 \end{cases}$$

2. $$T_{kers} = \begin{cases} \frac{P_m}{\omega_{kers}} & \text{if } T_{kers} < T_{max} \\ T_{max} & \text{if } T_{kers} > T_{max} \end{cases}$$

Remarks:

- The Currents I_1, I_2, I_3, I_4 will never be perfectly synchronized, so every current is added to the sum previously shown if and only if it becomes negative.

- Following this approach, the electrical losses on the motors due the Joule effect are neglected. In this way the energy used as reference is not the correct one and as a consequence, the amount of energy lost is absorbed from the grid in order to compensate.
  This issue can be treated in 2 different ways, explained in the following.

"Light Green" Approach:

Following this approach, the losses on the motors are not taken into account during the control, so the amount of energy injected in the Kers is composed partly by energy coming directly from the grid.

This solution is named "Light Green" since the energy stored in the kers is not totally the recovered one.

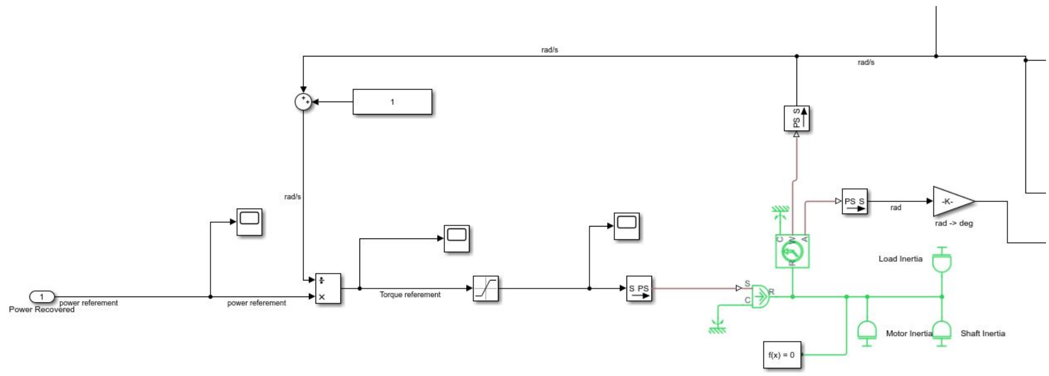

FIGURE 6.1: Light Green Approach Control Scheme of the Kers Group

The Kers control block takes the incoming mechanical power and then divide it by the actual velocity of the shaft. The result is the Torque T reference that the motor has to follow.

The control loop of the Torque has not been modeled since the parameters of the controller are the motor's electrical ones and are not accessible by the user in the used System. Furthermore, it has been assumed that the dynamic of this control loop is so fast that it can be neglected and the torque applied is always the right one.

The same concept is applied to the Lids Transfer Groups, so the power coming out is given just by the product of $T\omega$ neglecting the losses on the motors.

More Formal Description:

$$P_{kers} = \sum_{k=1}^{4} T_k \omega_k - P_{elect} + P_{elect} \tag{6.2}$$

Where:

- P_{elect} = Electrical Power Lost in the motors
- P_{elect} = Electrical Power Lost absorbed by the grid
- $P_{elect} = P_{elect}$

"Total Green" Approach:

The total green approach involves a model of the electrical losses both on the Lids Transfer groups and on the Kers Groups. Following this way, it is possible to have a better estimation of the energy that needs to be injected into the Kers.

The algorithm involves a continuous measurement of the currents and the corresponding model of the Electric Power Lost as:

$$P_{lost} = \frac{3}{2} R I^2 \tag{6.3}$$

This model is used both for the losses on the Lids Transfer motors and on the Kers motor.
Once that this power has been calculated, it is subtracted to the Mechanical one recovered and then the Torque T reference is continuously updated.

This approach is named "Total Green" because there is no energy absorbed by the grid and the Kers group is moved only with the recovered mechanical energy.

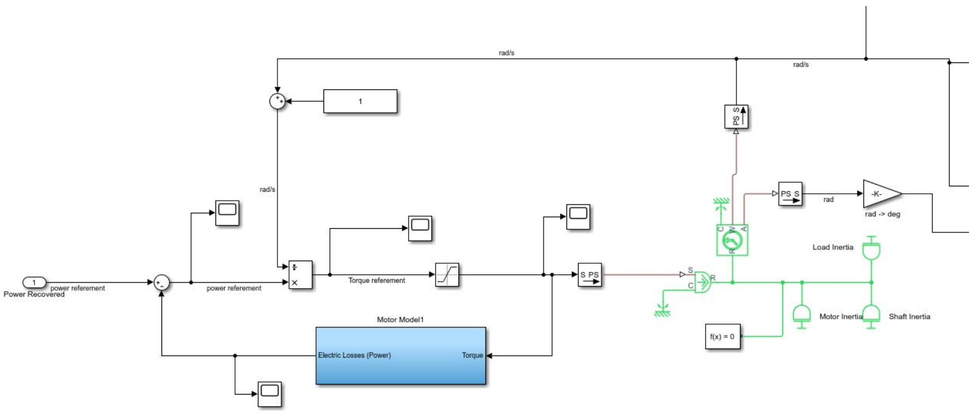

FIGURE 6.2: Total Green Approach Control Scheme of the Kers Group

More Formal Description:

$$P_{kers} = \sum_{k=1}^{4} T_k \omega_k - \sum_{k=1}^{4} \frac{3}{2} R_k I_k^2 - \frac{3}{2} R_{kers} I_{kers}^2 \tag{6.4}$$

Where:

- T_k, ω_k, R_k and I_k are referred to the Lids Transfer Groups
- $K \in [1, 4]$ is the number of Lids Transfer Group

Remark:

- Both in the "Total Green" and in the "Light Green" schemes it has been added a small negligible constant. This comes necessary because, at the beginning of the simulations, the velocity ω is zero and the division $\frac{P_m}{\omega}$ gives error.

By applying a "Total Green Approach", the simulations show that the needed amount of energy is stored in less then 8 minutes.

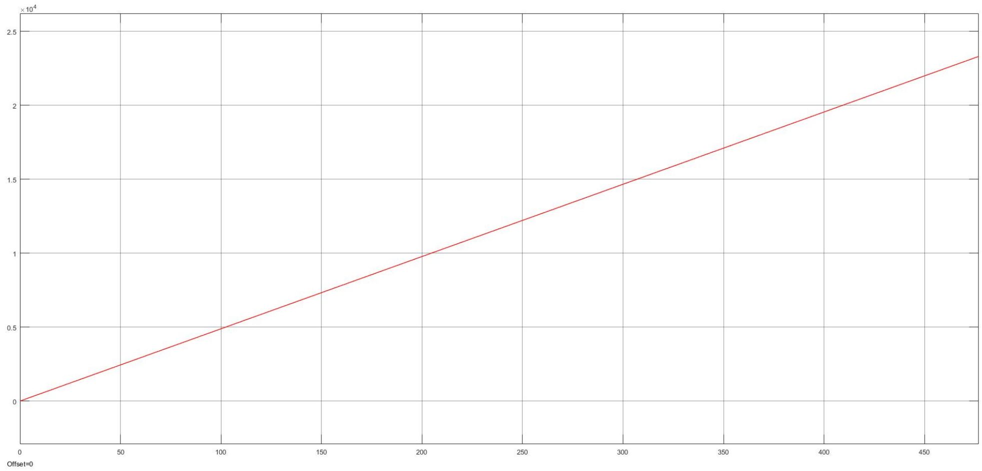

FIGURE 6.3: Energy accumulation during with a Total Green Approach

6.2 Energy Utilization Phase

During the Energy Utilization Phase the Kers Group needs to be braked in order to inject energy on the DC-Bus. In this way the other groups can have the needed power supply to perform the Emptying Phase of the machine.

The starting condition of this phase is that the Flywheel is rotating at the Steady State angular velocity(1600 rpm), that is calculated during the Flywheel Sizing phase.

The control of this phase needs to be very precise because, if not, 2 situations could take place:

- **Underflow of Energy:**
  In this situation the Kers is "Underbraked" with the consequence that the other groups have not the necessary energy to operate. In this condition, the Rockwell system stops all the machine until the main power supply is reestablished. If, for some reason, it is present a charge level into the driver's capacitance then the stop of the machine can be delayed by a few seconds. But the amount of energy stored in the driver's capacitances, even if they are fully charged, will not be sufficient for the emptying phase.

- **Overflow of Energy:**
  In this situation the Kers is "Overbraked", so the flow of energy injected on the DC-Bus is too high with respect to the one absorbed by the other groups.
  The first consequence is that the capacitance present in the driver will charge storing part of the energy. That could not be a problem at all since that energy will not be lost and, if the control corrects the brake, it could be reused.
  When the level of charge present in the capacitance rise to the limit, then the energy starts to be dissipated on the Braking Resistor also present in the driver. This situation needs to be absolutely avoided because the dissipation of the Kinetic Energy Recovered means a huge fall of the efficiency of the Kers System. In addition, it could happen that this dissipation causes an insufficiency of energy during the last phase of the Machine Emptying.
  If also the Braking Resistor reaches the Thermal Limit, then the Rockwell System stops braking the motor and shuts down the driver.

In the following, two different control strategies that have been considered and analyzed are presented.

6.2.1 Foreword Approach (Open Loop)

The first control approach that has been analyzed is the one that involves a Forward Control without feedbacks. In order to apply this control, it is necessary to have a very precise model of the system.

The key idea is that the Kers system has to be braked by applying a torque only on the base of the productivity of the machine. In this way, if the model of the machine is reliable, it can be possible to estimate the total amount of energy that the machine needs to operate time by time. Consequently, the Kers can be driven in order to inject on the DC-Bus the estimated amount of energy.
The only feedback measures that this type of control involves are the current and the angular velocity of the Kers. This is because the torque reference is calculated by the product $T\omega$ that needs to be balanced with the energy request by the machine.

The amount of energy that the machine needs is only an estimation based on the model with the productivity as input.
In this way, there's no guarantee that the estimated energy is the real one.

Since there is no feedback, this approach can be affected both by an underflow and an overflow on energy.

This approach has been abandoned since the hardware adopted allows an high number of measures and controls that can be used for more precise approach.

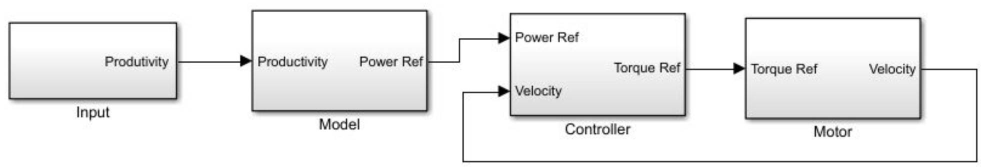

FIGURE 6.4: Control Scheme of the Open Loop Solution

6.2.2 DC Bus Approach (Closed Loop)

The DC-Bus approach is a safer one since the Kers is controlled with a feedback of the machine's energy consumption. The idea is to use a measure that can, time by time, represent the need of energy of the machine. In this way, the Kers system can be correctly controlled injecting on the DC-Bus the right amount of energy without the risk of an over or underflow phenomena.

The measure that better represents this idea is the value of the Voltage of the DC-Bus. Since all the machine's needed energy is absorbed through the DC-Bus, the voltage level will show if the flows of energy are balanced or not in a feasible way.
The capacitances present on the DC-Bus introduce a dynamic characteristic of it, therefore there is the need of an efficient control.

Since the nominal value of the DC-Bus's voltage is known (600V), it can be defined a control based on the voltage error.
As for the previous approach, the Kers will be controlled with a torque reference, but there is no more need of the loop referred to the angular velocity calculation since the input signal is not a power.

The controller must be saturated in order to allow the flow of energy only from the Kers to the DC-Bus and not viceversa. This is because in case, for example, of an overshoot of the Torque reference the Kers will not absorb energy from the DC-Bus. This phenomenon causes a drastic loss of efficiency of the Kers because energy is continuously passed from the Bus to the flywheel. If the system is not stable, iit can also occur that the oscillations cause huge damages both on the Kers and on the DC-Bus.

Unfortunately, the Rockwell documentation does not show the value of these capacitance so it has not been possible to perform a simulation in order to model the DC-Bus and tune a controller. Anyway the control scheme as been developed as follows:

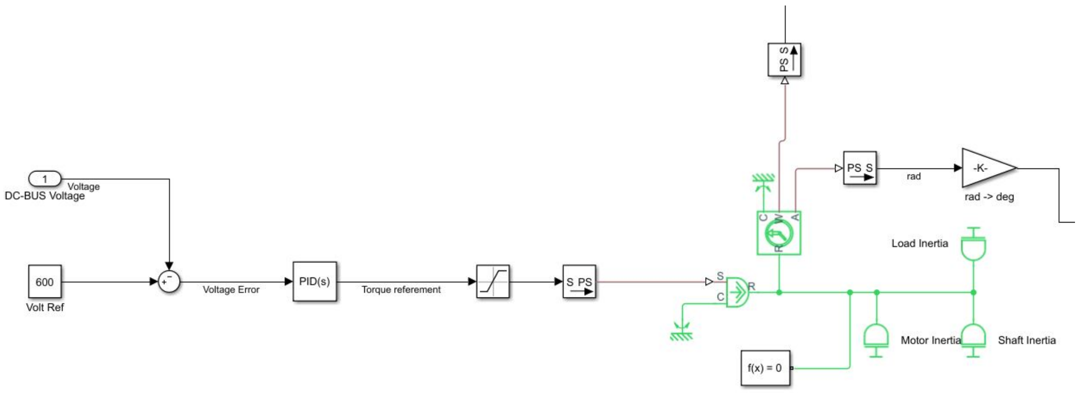

FIGURE 6.5: Controller of the Kers System with the DC-Bus approach

As shown, the voltage value is compared to the nominal one and a PID controller is applied in order to control the Torque.

Chapter 7

Conclusions (KERS VS UPS)

The developed system has shown that is possible to replace a UPS System with a more Green solution that performs the energy storing with a recovering process. The final analysis of the pro and cons of such system is:

Advantages

- **Flexibility:**
  This system, thanks to its simple structure, is very flexible and can be easily applied to all automation electronic platforms since it is independent from that. Also the amount of energy store can be easily modified just resizing the flywheel, and it makes the system applicable to a huge range of machines.

- **Cost:**
  The table shown in the System Realization section has shown that the cost of realization of this system is quite cheap. Those prices are referred to the realization of only 1 Kers System. If there will be an increase in the quantity, then the final cost will further decrease.

Component	Cost [€]
UPS System	6000
Kers System	~2000

  The Kers System's cost is about $\frac{1}{3}$ of the UPS's one.

- **Green Solution:**
  The scope of the project was to find a more green solution to provide an emergency power supply. The developed system uses only recovered energy to provide the power supply, while the UPS System uses only the power grid to charge itself.

- **Dimensions:**
  The dimensions of the Kers System are, despite what it seems, much lower than the UPS's ones. In particular the Kers System is about half of the UPS. The precise dimensions are explained in the following:

Component	Dimensions [mm]
UPS System	1300x650x335
Kers System	600x400x474

  As shown, the Kers system is significantly smaller than the UPS.

- **Control:**
  For what it regards the control, independently from what type of strategy is adopted, the Kers System provides in any case a better control than the UPS one. This is due to the fact that the UPS System is a "Plug and Play" device, which is built with the scope of being applied and work directly. The Kers System, thanks to the electronic structure implemented, allows a full control and it can be modified for every application.

Limitations

- **Single DC-Bus:**
  The machine on which is needed a Kers system needs to have a single DC-Bus or, at least, that all the drivers that needs an emergency power supply are on the same DC-Bus. This is due to the fact that this system operates on it, so if a machine has more than one, it could not be applied.
  If it is not possible to concentrate all the drivers on the same DC-Bus, then 2 different Kers Systems can be applied, one for each Bus. However, to apply this solution, there must be at least 1 group that can recover energy for each Bus.

- **Dynamic:**
  The machine on which the Kers has to be applied needs to have some groups with an high dynamic. As shown during the analysis, if there are no groups that can recover energy during the brakes then there is no energy to recover.
  In this case the only solution can be to "Charge" the Kers with the grid power supply, losing the Green approach.
  However, even if no kinetic energy can be recovered. The flywheel solution looks more flexible and integrated in the logic and motion control, with respect to UPS.

The development of this project led to a new type of system that is able to recover the kinetic energy of an automatic machine and to store it until it is necessary. The particular technologies and architecture of the system allow a full control and low production costs.
In conclusion, the objective to develop a more green solution to provide an emergency power supply has been achieved and the solution is ready to be physically implemented.

Chapter 8

Bibliography

Rockwell Automation – “Kinetix Rotary Motion Specifications”, Catalog, KNX-NX-TD001A-EN-PD001A-EN-P - F2017, Printed in the U.S.A., February 2017

Lenze – “Lenze Geared Motors and Smart Motors”, Catalog, V03-enGB-04/2015, Germany, 2015